Inês Alexandra Marreiros Silva

Degree in Biochemistry

Evaluation of Chemotherapeutic Potential of Natural Extracts Using 3D Models of Colon Cancer

Dissertation to obtain master degree in Biotechnology

Supervisor: Ana Teresa Serra, Ph.D, IBET/ITQB-UNL
Co-supervisor: Catarina Brito, Ph.D, IBET/ITQB-UNL

Jury:

President: Prof. Doutora Ana Cecília Afonso Roque
Arguer: Prof. Doutora Maria Paula Amaro de Castilho Duarte
Supervisor: Doutora Ana Teresa de Carvalho Negrão Serra

FACULDADE DE CIÊNCIAS E TECNOLOGIA
UNIVERSIDADE NOVA DE LISBOA

September, 2013

Inês Alexandra Marreiros Silva

Degree in Biochemistry

Evaluation of Chemotherapeutic Potential of Natural Extracts Using 3D Models of Colon Cancer

Dissertation to obtain master degree in
Biotechnology

Supervisor: Ana Teresa Serra, Ph.D, IBET/ITQB-UNL
Co-supervisor: Catarina Brito, Ph.D, IBET/ITQB-UNL

Jury:
President: Prof. Doutora Ana Cecília Afonso Roque
Arguer: Prof. Doutora Maria Paula Amaro de Castilho Duarte
Supervisor: Doutora Ana Teresa de Carvalho Negrão Serra

FACULDADE DE CIÊNCIAS E TECNOLOGIA
UNIVERSIDADE NOVA DE LISBOA

September, 2013

Copyright

Evaluation of Chemotherapeutic Potential of Natural Extracts Using 3D Models of Colon Cancer

Inês Alexandra Marreiros Silva

FCT/ UNL

UNL

Acknowledgments

Gostaria de expressar os meus sinceros agradecimentos a todos os que me apoiaram e contribuíram direta e indiretamente para o desenvolvimento deste trabalho.

Em primeiro lugar, à Doutora Ana Teresa Serra por todo o apoio e orientação prestada ao longo deste último ano. Agradeço por todo o acompanhamento, motivação e pelo apoio incondicional demonstrado mesmo nos momentos de maior adversidade. Obrigada por toda a contribuição para o meu desenvolvimento científico e pessoal.

Agradeço à Doutora Catarina Brito por me ter recebido e ter acreditado neste trabalho, pela disponibilidade e apoio, por tudo o que ensinou e por toda a ajuda prestada na procura de soluções no decorrer do trabalho.

À Doutora Catarina Duarte e Doutora Paula Alves por me terem dado a oportunidade de desenvolver o meu trabalho no laboratório de Nutracêuticos e Libertação Controlada e no laboratório de Tecnologia de Células Animais do IBET.

A todos os membros do grupo de Nutracêuticos e Libertação Controlada, especialmente ao Agostinho Alexandre, Mário Bordalo, à Ana Nunes, Joana Poejo, Sara Nunes e Janine Diogo agradeço por todo o apoio, comentários, sugestões e companhia. Agradeço à Doutora Maria do Rosário Bronze e à Elsa Mecha pela ajuda prestada na parte analítica.

Agradeço aos membros do laboratório de Tecnologia de Células Animais, Marta Silva e Ana Paula Terrasso por a ajuda e tempo despendido. Um especial agradecimento à Marta Estrada por todo o conhecimento transmitido e pela grande contribuição para o desenvolvimento de uma importante fase deste trabalho, agradeço muito todo o auxílio, paciência e todo o tempo despendido comigo.

Agradeço a todos os meus amigos próximos e aos meus colegas de tese ITQB, foram mesmo um grande apoio, como vocês por perto tudo se tornou mais fácil.

À minha família pelo apoio, foram fundamentais para que eu me tornasse a pessoa que sou hoje, e um muito obrigado por me terem proporcionado a minha formação académica.

Por fim, um enorme agradecimento ao Filipe por toda a compreensão, companheirismo e paciência. A tua motivação e ajuda foram fundamentais neste ano, obrigada por teres sempre acreditado em mim.

Abstract

Recently there is a growing interest in cancer treatment through the use of natural compounds. In particular, phenolic compounds and monoterpenes found in fruits and vegetables are very attractive in the prevention and chemotherapy of various types of cancer. However, many promising compounds previously tested in *in vitro* cell models fail to demonstrate activity when evaluated *in vivo*. Therefore, there is an emerging need to develop more robust and reliable cellular models for pre-clinical evaluation of new chemotherapeutic agents.

The main goal of this thesis was the evaluation of the chemotherapeutic potential of natural extracts, rich in bioactive compounds, using 3D models of colon cancer. For this purpose, a 3D model of human colorectal cancer cell line HT29 was developed.

By culturing HT29 cells in a stirred culture system, it was possible to obtain 3D cellular spheroids with different size diameter during culture time. It was verified phenotypic changes within the spheroid along culture, such as formation of apoptotic core and altered expression of stem and epithelial markers in different spheroid areas, which are typical features of tumor progression.

After an initial screening of the antiproliferative potential of 14 natural extracts performed in a 2D model of HT29 cells, the most promising samples were selected for further analysis in the 3D model. Cherry and orange extracts showed potential anticancer effect in HT29 aggregates through the inhibition of cell proliferation, induction of apoptosis and cell cycle arrest. A decrease on the bioactive effect was verified with the increase of aggregate diameter, probably due to limited diffusion. The anticancer activity was correlated with the phytochemical composition of natural extracts. For cherry extract, perillyl alcohol was the main bioactive compound identified whereas for orange extract, compounds like nobiletin, tangeretin and sinensetin were highlighted.

Results of this thesis demonstrated that natural extracts of cherry and orange contain bioactive molecules with promising application on the development of new therapies for colon cancer treatment. The use of 3D cell models is a valuable tool for the study and evaluation of the effect of new chemotherapeutic compounds.

Key words: 3D cell models; Colon cancer; Natural extracts; Phytochemicals; Chemotherapy

Resumo

Recentemente tem surgido um interesse crescente no tratamento de cancro através do uso de compostos naturais. Nomeadamente, os compostos fenólicos e os monoterpenos, presentes em frutas e vegetais, são muito atrativos na prevenção e quimioterapia de diversos tipos de cancro. Muitos dos compostos promissores, previamente testados em modelos celulares *in vitro*, apresentam falhas quando avaliados *in vivo*. Como tal, existe uma necessidade emergente de desenvolvimento de novos modelos celulares, mais robustos e mais representativos do tecido *in vivo*, para avaliação pré-clínica de novos agentes quimioterapêuticos.

Neste trabalho pretendeu-se avaliar o potencial quimioterapêutico de extratos naturais, ricos em compostos bioativos, usando modelos 3D de cancro do colon. Para tal, foi necessário proceder ao desenvolvimento do modelo usando uma linha celular humana de cancro do colon (HT29).

Foi possível obter, com reprodutibilidade, um modelo celular 3D (agregados) de cancro do colon usando um sistema de cultura agitado, tendo estes apresentado um fenótipo variável ao logo do tempo de cultura. Estas alterações, tais como, a formação de um centro apoptótico e alterações na expressão de marcadores estaminais e epiteliais, são também características da progressão tumoral.

Após um estudo inicial onde foi avaliada a capacidade antiproliferativa de 14 extratos naturais num modelo 2D de células HT29, foram selecionadas as amostras mais promissoras para posterior análise no modelo 3D. Os extratos de cereja e laranja apresentaram potencial efeito anticancerígeno no novo modelo desenvolvido, através da inibição da proliferação celular, da indução da apoptose e paragem do ciclo celular, tendo-se registado uma diminuição do efeito bioativo com o aumento do agregado. A atividade anticancerígena foi correlacionada com a composição fitoquímica dos extratos. Para o extrato de cereja foi enfatizada a relevância do álcool perílico e, no caso, do extrato de laranja, compostos como a nobiletina, tangeretina e sinensetina foram destacados.

Os resultados obtidos demonstraram o potencial promissor dos compostos naturais no desenvolvimento de novas terapias aplicadas ao tratamento do cancro do colon. O uso de modelos celulares em 3D constitui uma boa ferramenta para o estudo e avaliação do efeito quimioterapêutico de novos compostos.

Palavras-chave: Modelos celulares em 3D; Cancro do colon; Extratos naturais; Fitoquímicos; Quimioterapia

Contents

Figure Index

Table Index

Abbreviations

ABC	ATP binding cassette
Ajs	Adherens junctions
APC	Adenomatous polyposis coli
ATP	Adenosine triphosphate
CK	Cytokeratin
CDK	Cyclin-dependent kinase
CSC	Cancer stem cell
CSE	Conventional solvent extraction
DAD	Diode array detector
DNA	Deoxyribonucleic acid
DAPI	4',6-diamidino-2-phenylindole
ECM	Extracellular matrix
EC50	Half maximal effective concentration
EDTA	Ethylenediamine tetraacetic acid
EMT	Epithelial-mesenchymal transition
EtOH	Ethanol
FACS	Fluorescence activated cell sorting
FAP	Familial adenomatous polyposis
FBS	Fetal bovine serum
FDA	Fluorescein diacetate
FITC	Fluorescein isothiocyanate
FSG	Fish skin gelatin
GAE	Gallic acid equivalent
HNPCC	Hereditary nonpolyposis colon cancer
HPLC	High performance liquid chromatography
K	Kelvin degree
MCTS	Multicellular tumor spheroid

mg/ml	Milligrams per mililiter
mM	Milimolar
MMP	Metalloproteinase
MMR	Mismatch repair
MPa	Mega Pascal
OE	Oleuropein equivalent
PBS	Phosphate saline buffer
PE	R-Phycoerythrin
PFA	Paraformaldehyde
PI	Propidium iodide
PMFs	Polymethoxylated flavones
PLL	Poly-L-lysine
POH	Perillyl alcohol
ROS	Reactive oxygen species
RPMI	Roswell Park Memorial Institute medium
RWV	Rotating-wall vessel
SD	Standard deviation
TLC	Thin layer chromatography
TPC	Total phenolic content
VEGF	Vascular endothelial growth factor
v/v	Volume per volume
w/v	Weight per volume
µl	Microliter
µm	Micrometer
^{0}C	Celsius degree

1 Introduction

1.1 Colon Cancer

Cancer is the primary cause of death in economically developed countries and the second in developing countries, representing around 13% (7.6 million) of total deaths. Most of these deaths are due to lung, stomach, liver, colon and breast cancer [1].

Particularly, colon cancer is one of the most common and lethal diseases in developed countries (Figure 1.1), being the third most common cause of cancer in men and the second cause in women worldwide. In Europe, this malignancy kills 230,000 citizens every year and it is the second most common malignant tumor. Colon cancer continuous to be one of the most incident cancers, however, over the past 10 years, death rates have declined 3% in US [2].

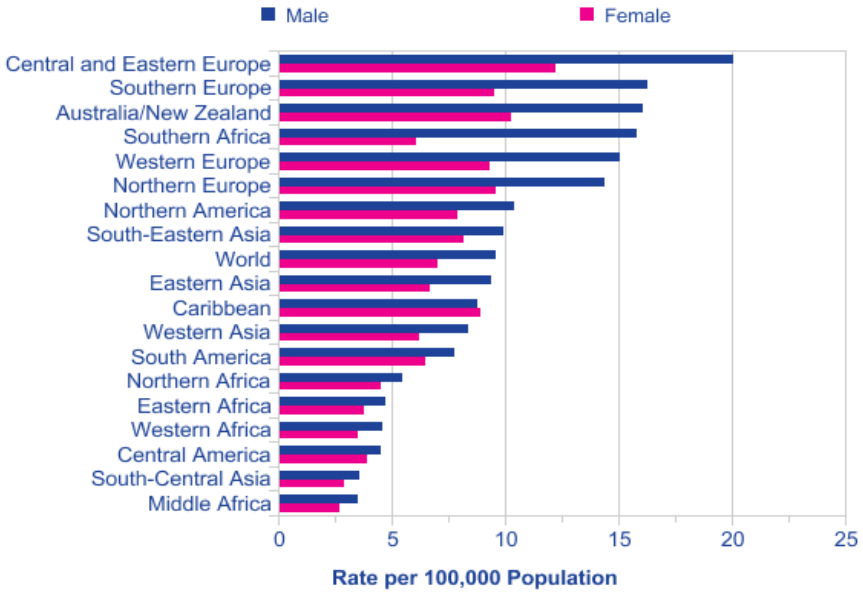

Figure 1.1: World age-standardized mortality rates of colorectal cancer, 2008 data [3].

Colon is a muscular tube with about 150 centimeters which absorbs water and salt from the lumen. Colon has 4 sections, including ascending, transverse, descending and sigmoid colon. The layers of the large intestine are mucosa, submucosa, muscularis and serosa [4]. Human colon mucosa is made from a single sheet of columnar epithelial cells, which form invaginations into the underlying connective tissue, constituting the basic functional unit of the intestine, the crypt. Colon is formed by millions of crypts and evidences document the presence of a stem-cell population at the base of the crypt [5]. These stem cells present a key role in intestinal regeneration, however, they can acquire mutations that can lead to malignancy. Stem cells of colonic crypt present as natural targets of transformation, due to

their longevity and self-renewing capacity [6]. Apoptosis is a crucial mechanism to control and promote normal crypt homeostasis [7].

Colon cancer arises from colon cells and can be designated colorectal cancer, if neoplasms are found from caecum to rectum. This abnormal growth of cells caused by several gene mutations, result in a dysregulated balance between cell proliferation and death. Ultimately, these cells can invade tissues and metastasize to distant sites which is typical from malignant cancer cells [8].

The development of colon cancer can occur with different proliferation rates, but, in general, it is a slow process that evolves several years. Most cases begin as polyps, which are benign tumors made from the excessive proliferation of the inner lining cells. Some polyps remain as non-cancerous tumors (hiperplastic and inflammatory polyps) and others can evolve into a pre-malignant type, designated as adenoma or adenomatous polyps. This type of polyps originates adenocarcinomas (malignant type), which represents more than 98% of total colorectal cancers (Figure 1.2). These tumors arise from glandular epithelial cells of mucosa, which produces mucus that lubricates the lumen of the large bowel. Adenocarcinoma formation process can take 5-10 years to occur and only around 10% of adenomas become cancer [9]. There are other types of colon tumors which are less prevalent, such as carcinoid and gastrointestinal stromal tumors, lymphomas and sarcomas [10]

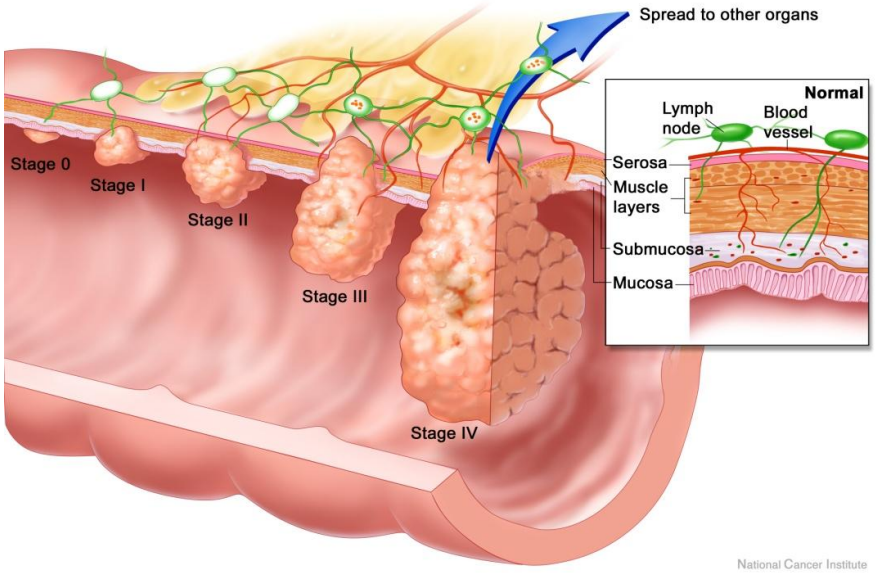

Figure 1.2: Colorectal adenocarcinoma progression stages. The lower stage indicates a smaller tumor with less proliferation and the higher stage represents a bigger tumor with invasion (adapted from National Cancer Institute) [11].

The sporadic type of colon cancer, which is the most common, arises from the accumulation of genetic mutations. Carcinogenesis is a long and multistep process, which comprises irregular genetic modifications. Fearon and Vogelstein (1990) have proposed a genetic model for colon carcinogenesis creating a correlation between genetic events and tissue morphology [12]. In order to start the malignant formation it is required the mutation of a cascade of genes. This cascade starts when Adenomatous Polyposis Coli gene (*APC*), a tumor

suppressor gene, becomes inactivated by mutation. Then, it progresses with more genetic mutations in other tumor-suppressing genes such as *K-ras* (Figure 1.3). This events, combined with DNA modulation by methylation, leads to the inactivation of repair genes or the amplification of oncogenes activation. All these genetic damages are morphologically related with the developing process of polpys and adenomas [13].

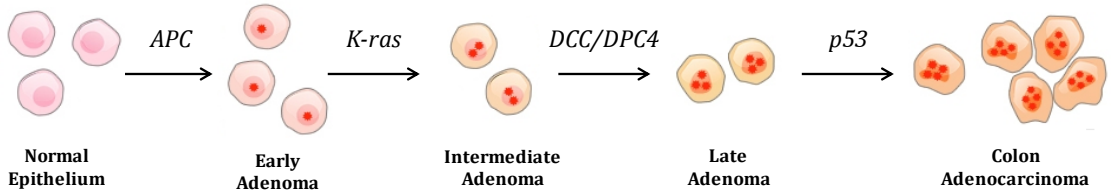

Figure 1.3: Multiple step model of sporadic colorectal carcinogenesis and progression (adapted from [8]).

One prominent genetic change occurs in *p53*, a tumor suppressor gene. The *p53* has been implicated in 80% of sporadic colon cancer cases. It is the most frequently mutated gene found in solid tumors [14]. Other tumor suppressor genes have been reported, such as *MCC*, *DCC* and *DPC-4* [15].

1.1.1 Risk Factors

As mention above, developed countries appears to have a higher incidence of colon cancer and it can be linked with modern diet (high dietary intake of fat, refined carbohydrates, animal protein and low intake of fiber) and lifestyle, combined with lack of physical activity [16]. The majority of colon cancer cases are sporadic, which mean that they are not related to genetic inheritance or family history. The major risk factor is age and, in fact, 90% of these tumors are diagnosed after the age of 50 years. This profile may be due to a lifetime of biochemical injuries resulting from the risk factors previously described. Other risk factors involved in sporadic type includes: prior personal colon cancer history, inflammatory bowel disease, radiation exposition and acromegaly [17].

Another strong factor for the development of colorectal cancer is the genetic predisposition. There are two known genetically inherited syndromes: familial adenomatous polyposis (FAP) and hereditary non-polyposis colon cancer (HNPCC). These are the most common familial colon cancer syndromes, but together they account for only about 5% of colorectal cancer cases [18]. HNPCC can be caused by a mutation in one of several DNA mismatch repair (MMR) genes. MMR system prevents incorrect base pairing and when they are inactivated there is an accumulation of spontaneous mutations in DNA microsatellites [17]. FAP is the most characterized familial syndrome and it is caused by the mutation of the *APC* gene [17].

1.1.2 Metastization

Metastasis is the dissemination of malignant cells from the primary tumor to a distant organ and it constitutes the leading cause of death for cancer patients. It is a complex molecular mechanism that includes cancer cell migration and invasion into adjacent tissues and intravasation (cells enter in blood space to travel to distant organs) into blood/ lymphatic vessels [19]. Despite the clinical importance, the biological process of metastasis remains poorly understood. However, several studies have shown that tumor cells penetrate adjacent tissues by different ways. They can disseminate as individual cells, such as leukemia, lymphomas and most solid stromal tumors, or they can expand in solid cell strands, sheets files or clusters, commonly observed in epithelial tumors. Usually, the lower differentiation stages are more likely to spread by individual cells [20].

Metastasis formation involves a multiple step process. First, there is the development of a blood supply that can support the metabolic demands, a process called angiogenesis. These new blood vessels provide a route by which the malignant cells can escape from the primary tumor and enter into the blood stream. Cancer cells can also get access into circulatory system indirectly, through the lymphatic system. Once in the circulation, they extravasate to the surrounding tissue, starting a new proliferation process (Figure 1.4) [21]. During the invasion process, cancer cells penetrate the basement membrane and interstitial stroma through proteolysis of extracellular matrix (ECM). Metalloproteinases (MMPs) play a crucial role for this EMC proteolysis [22].

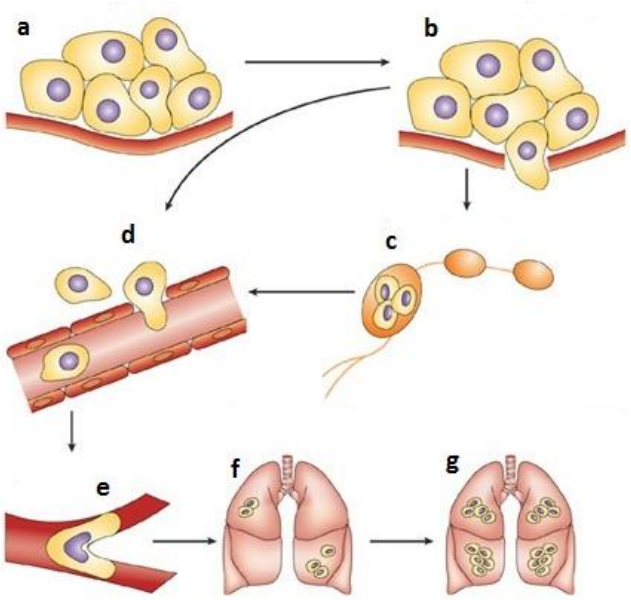

Figure 1.4: Metastatic process schematization. (**a**) *in situ* cancer. (**b**) invasion begins with changes in cell-cell and cell-EMC adherence, destruction of stroma and motility. The cells can migrate (**c**) via lymphatic or (**d**) directly in the blood circulation. (**e**) survival, arrest of metastatic cancer cells and extravasation of circulatory system. (**f**) colonization of distant organs which might remain inactive for years, occulting micrometastases and (**g**) growing of secondary tumor and angiogenesis [23].

Epithelial-mesenchymal transition (EMT) plays an important role in the invasive cascade because it marks the transition from a collective to a single-cell migration mechanism. The development of metastasis requires the movement of cancer cells, driving the progression of carcinomas to an invasive and metastatic phonotype. In general, EMT process occurs during embryonic development in order to escape from structural constraints imposed by tissue architecture, adopting a more flexible cell movement capacity. Briefly, during EMT, epithelial cancer cells lose their polarity and some cell-cell and cell-ECM adhesion systems, resulting in reduced intercellular interactions and increased migratory character as mesenchymal cells. In the metastatic process, EMT enables cancer cells to disseminate from a primary tumor and promotes their self-renewal, required for metastases progression. The loss of expression of structural epithelial proteins (E-cadherin, plakoglobin and cytokeratins) was verified, when epithelial cells become invasive. E-cadherin is an adhesion molecule essential for the maintenance of adherents junctions, thus, the loss of their expression is a hallmark characteristic of EMT [24]. These phenotypic alterations, in general, are accompanied by the expression of vimentin and other mesenchymal characteristic proteins [25]. In Table 1.1 are summarize the main phenotypic alterations associated with EMT in colon carcinoma.

Table 1.1: Phenotypic alterations associated with EMT in colorectal carcinoma [25].

	Epithelial	**Mesenchymal**
Polarization	Polarized with differences between apical and basal membrane constituents	No apical-basal membrane polarity, elongated morphology
Cell-cell contacts	Strong cell-cell junctions as tight and adherent and desmosomes	Weak cell-cell contacts discernible
Structural proteins	E-cadherin, cytokeratins	Vimentin
Extracellular environment	Basement membrane containing type IV collagen and laminin	Expression of type I collagen, fibronectin and metalloproteinases
Motility	Non-motile cells	Highly motile cells often displaying active Wnt/β-catenin

The role of β-catenin in E-cadherin-mediated cell-cell adhesion is essential for the study of the molecular basis of EMT and malignant cancer development. In colon epithelia, β-catenin links E-cadherin to the actin in cytoskeleton. The dismantling of cell-cell adhesion (loss of E-cadherin) during EMT releases β-catenin which displays an important role in the regulation of EMT. Indeed, it is usual to find β-catenin accumulation in the cell nucleus of the invasive carcinoma cells, instead of being located in the plasmatic membrane [25].

Once cancer cells have been established in the tissue, the new stroma environment lacks signaling to undergo an EMT. This allows cancer cells to revert the prior process and occurs

a mesenchymal-epithelial transition [26]. Thus, EMT process makes possible cancer cell dissemination and enables a self-renewal capacity to metastatic cancer cells [27].

1.1.3 Chemotherapy

The success of chemotherapy in the treatment of malignant diseases has been dramatic. In the most common carcinomas (breast, colon and lung) the effectiveness of chemotherapeutic agents has been disappointing [28].

Usually, cancer therapies, including surgery, chemotherapy and radiotherapy, have a limited but important role in the overall treatment of most solid tumors. In early-stage disease, low risk patients are often cured with surgery alone, but in many other cases a combination of treatments is required. The use of combined therapies or agents, which act through different molecular mechanisms, has been considered as a promising strategy [29]. These mechanisms are summarized in Figure 1.5.

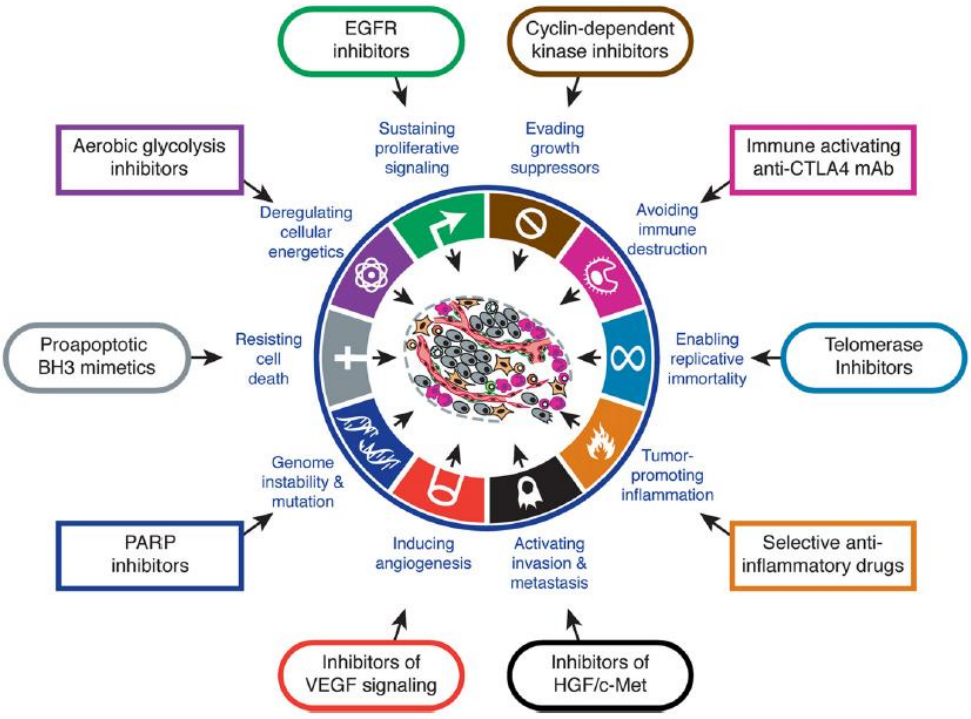

Figure 1.5: Therapeutic targeting of the Hallmarks of Cancer. Drugs that interfere with each of the acquired abilities necessary for tumor growth and progression have been developed and are in clinical trials [30].

In recent years, it has been achieved great improvements in the knowledge of intracellular mechanisms, which are involved in cell cycle deregulation and the response of cancer cells to external growth factors. Cancer cells differ from normal cells due to their ability to grow and survive. The accumulation of mutations on proto-oncogenes and tumor suppressor genes promote cell division and generate insensitivity to growth inhibitory signals.

Chemotherapy drugs cause apoptosis by directly interfering with DNA or by targeting the key proteins involved in cell division [31].

Cell cycle is controlled by several checkpoints. These points are regulated by the transient association of cyclin and cyclin-depend kinase in order to determine the progression into next stage of division. Cyclins appear to act as oncogenes in some type of cancers. Hence, there are multiples aberrant pathways which can be exploited by drug design. In addition, different phases of the cell cycle or different signaling pathways are targeted to achieve maximal cell kill and the less likelihood of resistance [31, 32].

The most successful drug used in chemotherapy of colon cancer is 5-fluorouracil (5-FU). Particularly, this type of cancer is usually treated with a combinatory therapy with other drugs. It has been reported various mechanisms of action, including inhibition of thymidylate synthase and incorporation into RNA and DNA. Pyrimidine *de novo* synthesis is impossible without thymidylate synthase activity and their inhibition results in a decrease of DNA synthesis and repair [33].

In general, standard anticancer drugs show low efficacy in providing long term resolutions in epithelial tumors. Recently, this limited effectiveness of anticancer therapies has been attributed to the existence of cancer stem cells (CSCs), which confers a highly drug resistant phenotype to the tumor. CSCs are characterized by their unlimited ability to self-renew, to be undifferentiated and seed new tumors with the same cellular heterogeneity. In the metastasis process, disseminated cancer cells require self-renewal capability, very similar to that exhibited by stem cells, in order to generate metastases in distant parts of the body [27]. Further, it is believed that common chemotherapy kills most cells in a tumor but leaves CSCs behind. It has already been shown that drug transporters protect CSCs from chemotherapeutic agents. This drug's resistance mechanism is due to the expression of high levels of specific ATP-binding cassettes (ABC) drug transporters which have roles in the transport of drugs across the cells. Other stem cells properties that provide a long lifespan include the relative quiescence, an active DNA-repair capacity and resistance to apoptosis [34].

1.2 Natural compounds and colon cancer

Over 200 years ago, Friedrich Sertäurner, a pharmacist´s apprentice, isolated the first pharmacologically active pure compound from a plant. This compound was morphine from opium, produced by cutting the seed pods of the poppy, *Papaver somniferum* [35]. After this event, it was started a new era where drugs from plants could be purified, studied and administered. In 1990 about 80% of drugs were natural products or analogs inspired by them, causing a revolution in medicine. However, during the 90's, it was observed an expansion in the synthetic medicinal chemistry, driving to a decrease of proportion of new drugs based on natural products to 50% [36, 37]. Nevertheless, natural products continue to provide unique structural diversity in analogy to standard chemistry. Since less than 10% of world's biodiversity has been evaluated for potential biological activity, many useful natural compounds await discovery [38].

The World Health Organization estimates that 80% of worldwide population chooses traditional medicine for primary health care [39]. Essential oils from plants, nutraceutical products, dietary supplements, herbal remedies, teas and infusions are the main selected products [36].

As a source of new pharmaceuticals, natural products and derived molecules play an important role due to the great variety of functionally relevant metabolites of microbial and plant species. The development of improved products and new drugs can provide to drug development the scientific tools needed to perform a robust study of natural compounds and traditional medicines [40]. To be eligible as a medicinal plant or compound, it is necessary to take considerations about phytochemical analysis and pharmacological screening, which includes studies *in vitro* and in animal models. It needs further verification in order to identify the most bioactive components and their mechanisms of action, activity and cytotoxicity profiles. In 2008, over 100 natural products-derived compounds were undergoing clinical trials and, at least, 100 products in preclinical development. Most of them were derived from plants and microbial sources and these products were predominantly being study for the use in cancer or as anti-infectious agents[36, 41].

In the context of colon cancer, multiple natural products and their bioactive phytochemicals have been found to exert anticancer effects by inducing cell-cycle arrest and apoptosis, decreasing cell proliferation and angiogenesis while inhibiting cancer cell invasion and migration. Besides, phytochemical compounds can also modulate several signals transduction and pathways involved in colon cancer development, including COX-2/PGE2 and Wnt/β-catenin [42]. Various *in vitro* studies in a wide range of colon cancer cell lines have shown the chemopreventive and chemotherapeutic effects of natural products and their constituents (Figure 1.6) [43]. In addition, *in vivo* studies using experimental carcinogenesis models have also been reported for the same natural products [44, 45].

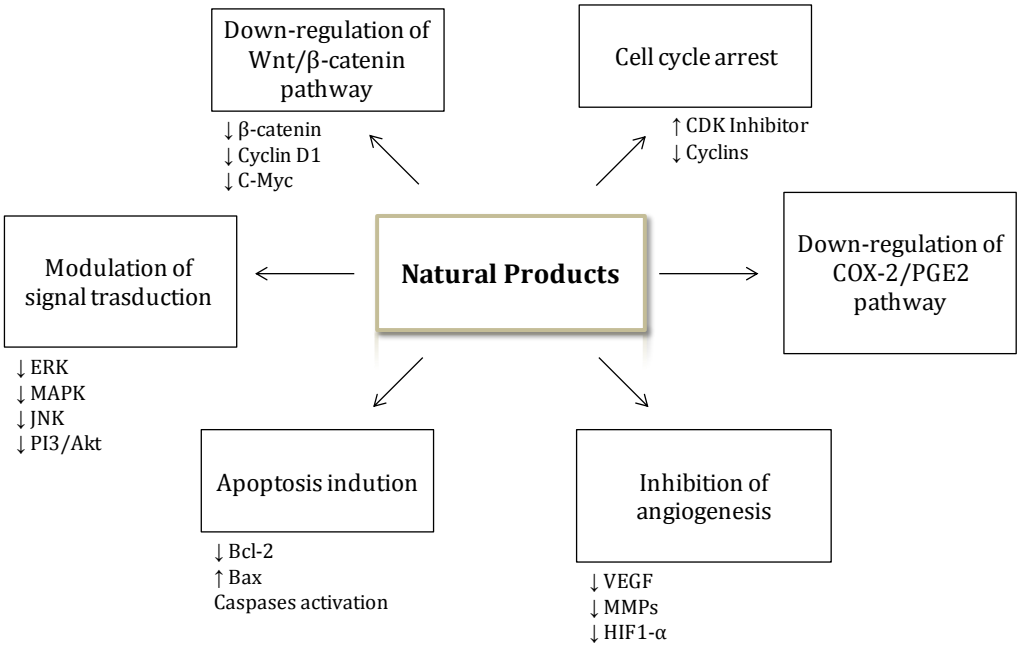

Figure 1.6: Different mechanisms of action of natural products in colon cancer prevention and therapy (adapted from [43]).

Several developments in organic chemistry have been inspired by natural products, including the advances in methodologies and the possibility for synthesizing analogues of the original compound with enhanced pharmacological proprieties [46]. Natural products can provide 'privileged' structures in terms of their ability to be the basis of new drugs. Natural products libraries are basically based on 3 major groups of phytochemical compounds, namely alkaloids, phenolics and terpenoids. The application of several techniques allows the creation of analogues and derivatives of these phytochemical compounds, with the possibility of being patented. Actually, with the development of analytical techniques, it has become easy to isolate, purify and determine structures of relevant compounds present in natural products [36].

Phenolic compounds, found in a large variety of plants, have shown to inhibit or attenuate the initiation, progression and spread of cancer cells, both *in vitro* and in animal models *in vivo*. This phytochemicals are secondary metabolites and can be monophenolic (one phenolic aromatic ring) or polyphenolic (more than one aromatic ring). Up to now, over 8000 different phenolics in plants were identified and classified in multiple sub groups of compounds (Figure 1.7). Flavonoids are the most abundant and numerous plant phenolics and can be found in high concentrations in the leaf epidermis and fruit skins due to their important role in pigmentation, UV protection and disease [47].

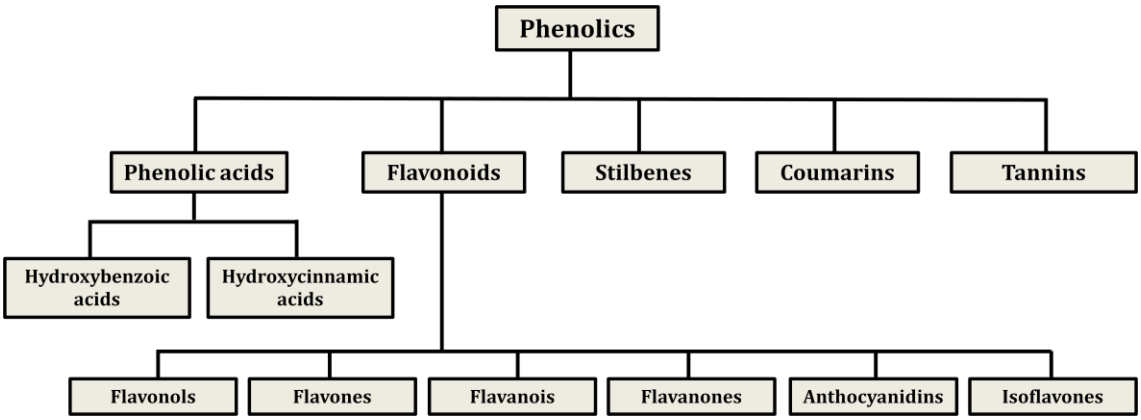

Figure 1.7: Schematic classification of phenolic compounds reported to have health benefits (adapted from [47]).

Phenolic compounds play a significant role in the suppression of tumor initiation, as well as in the promotion and progression of cancer. They can act in the regulation of growth factors-receptor interactions and in cell signaling cascades, such as kinases and transcription factors, which determines cell cycle arrest, cell survival and apoptosis. Aberrant growth factor expression results in an uncontrolled cell proliferation. Furthermore, phenolic compounds can enhance immune system to recognize and destroy cancer cells, inhibit angiogenesis and reduce the metastatic potential. The antiangiogenic effect appears to be linked with attenuation of MMPs and inhibition of vascular endothelial growth factor (VEGF) [47].

Terpenoids or terpenes are the largest group of natural compounds and many of them present bioactivity in the treatment of human diseases. Among the terpene-based pharmaceuticals already commercialized, it can be found a successful anticancer drug, the Taxol®. Besides anticancer properties, terpenes display a wide range of other biological activities against inflammation and infectious diseases. They can be structurally classified as monoterpenes (C_{10}), sesquiterpenes (C_{15}), diterpenes (C_{20}) and sesterterpenes (C_{25}) [48].

Monoterpenes are nonnutritive constituents of the essential oils of citrus fruits, cherry, mint and herbs. Antitumor activity of several monoterpenes was extensively reported [49]. Limonene, carvone and perillyl alcohol are the most interesting molecules as chemopreventive and chemotherapeutic agents against tumor cells. The mechanism of action is mainly related with the induction of apoptosis and the interference with key regulatory proteins (Figure 1.8) [48, 49].

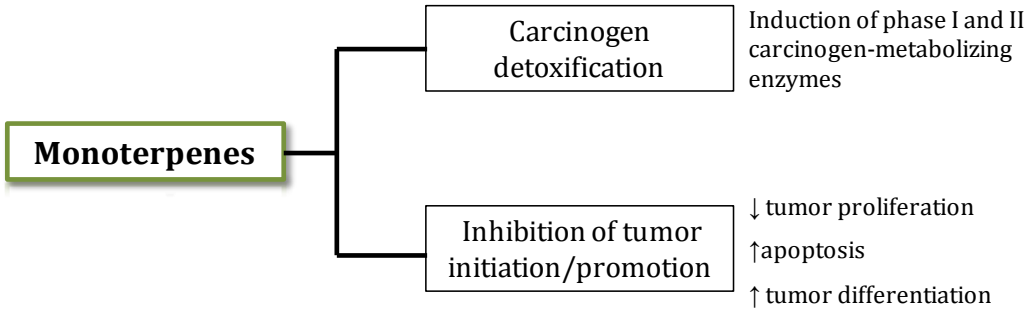

Figure 1.8: Actions of monoterpenes in cancer prevention and therapy [49].

Alkaloids are a diverse group of compounds that contain one or more nitrogen atoms, usually, in a heterocyclic ring. They are widely distributed in the plant kingdom, mainly in higher plants. Alkaloids are among the most important bioactive components and some of them have already been successful in cancer chemotherapy [50]. *Vinca* alkaloids (vinablastine, vincristine and vinerolbine) isolated from Madagascar periwinkle are anticancer agents in clinical use [51]. Recently, other anticancer relevant alkaloids have been studied, such as berberine, matrine and evodiamine. They act in several cancer mechanisms, including apoptosis, cell cycle arrest, angiogenesis, metastasis, and others [50].

Despite a period of decrease in their use, there are multiple natural compounds candidates for new drugs in current development. Phytochemical compounds provide the core scaffolds for future drugs due to an increasing acceptance of public opinion. In the future, the continuing development of natural products and chemical libraries based on natural products will continue to grow in drug research [36].

Several fruits have been reported as strong sources of phytochemical compounds, as previously described. The high content in these potential anticancer compounds makes this natural extracts as having therapeutic interest. The use of the fruit wastes as a source of bioactive compounds might be an approach to recover phenolic compounds and terpenoids. Fruits as olives, oranges, plums, peaches and cherries present several anticancer molecules that can be selectively extracted in order to obtain an extract with anticancer activity [52-55].

1.2.1 Olive

Olive tree (*Oleaceae*) has a great economic and social role in Mediterranean countries and it is one of the most important agricultural activities in this area. Oil and olives are the main products of olive-related industry, which generates large volumes of by-products such as crude olive cake, vegetation water, twigs and leaves [56, 57]. Olive products have shown beneficial effects on human health mostly due to the presence of antioxidants such as phenolic compounds, carotenoids and tocopherols that assume an important function in disease prevention [58, 59]. Studies demonstrate the presence of anticancer active phenolics in olive fruit, including, luteolin, apigenin, oleuropein, rutin and hydroxytyrosol (Table 1.2) [60]. The anti-colon cancer activity of olive fruit skin terpenoids-rich extracts have been also reported [61].

The stone represents 18-22% of total olive weight. It is mainly formed by lignocellulosic material with commercial interest for production of solid, liquid or gas biofuel. Despite the relevance for the biofuel industry, olive stone is a rich source of valuable components due to their chemical and physical properties. Like the olive fruits, the presence of phenolic compounds in olive seed is also important. Several anticancer compounds have been already identified, including, tyrosol, oleuropeina and their derivatives (Table 1.2) [62].

Table 1.2: Reported anticancer activity of phenolic compounds from olive.

Phenolics	Mechanism of anticancer activity	Cancer model	Ref
Tyrosol	↑ apoptosis	*in vitro* (cell-based assays)	[63]
Hydroxytyrosol	G1 arrest, ↑ apoptosis, ↓ ROS	*in vitro* (cell-based assays)	[63]
Oleuropein	S arrest, ↓cell proliferation, ↓ invasion, ↓ migration, angiogenesis inhibition	*in vitro* (cell-based assays) *in vivo* (mouse model)	[64, 65]
Verbascoside	↓ ROS, ↑ tumor differentiation	*in vitro* (cell-based assays)	[66, 67]
Apigenin	G2/M arrest, ↓cell proliferation, ↑ apoptosis, carcinogens detoxification	*in vitro* (cell-based assays) *in vivo* (mouse model)	[68-70]
Luteolin	↓ ROS, G2/M arrest, ↓cell proliferation, ↑ apoptosis, angiogenesis inhibition, carcinogens detoxification	*in vitro* (cell-based assays) *in vivo* (mouse model)	[71, 72]

1.2.2 Orange

Citrus fruits have commercial relevance due to their nutritional value and special flavor. About 34% of orange production was used for juice production, where a large amount of residues is produced, constituted mainly by orange peels [52]. Thus, large amounts of peels are produced every year; this residue is the primary waste fraction.

Sweet orange (*Citrus sinensis*) peel is an interesting source of phenolic compounds such as polymethoxylated flavonoids and terpenoids, mainly limonene and linalool [52]. Polymethoxyflavones (PMFs) have been of particular interest because these flavonoids display a large spectrum of biological activities, including, anti-inflammatory, anticancer (Table 1.3) and antioxidant. These compounds are particularly abundant in sweet orange [73-76]. PMFs are lipophilic molecules due to the hydrophobic nature of methoxy groups, in comparison to hydroxyl groups, as observed in quercetin, luteolin and narigenin. Consequently, PMFs have shown a higher absorbance through the small intestine and are easily absorbed into the blood circulation system [52]. All of these beneficial actions suggest new value-added uses for these compounds as nutraceuticals, generating considerable interest to the citrus industry.

Tangeretin and nobiletin are among the most effective citrus flavonoids at inhibition of human cancer cell proliferation [70]. In addition, *in vivo* antitumor studies of PMFs reveal their safe pharmacological use [73].

Table 1.3: Reported anticancer activity of orange peel flavonoids.

Flavonoids	Mechanism of anticancer activity	Cancer model	Ref
Tangeretin	G1 arrest, ↓↓cell proliferation, cytostatic, ↓tumor invasion, ↑ tumor differentiation	*in vitro* (cell-based assays) *in vivo* (rat model)	[73, 77]
Nobiletin	G1 arrest, ↓↓cell proliferation, ↑ apoptosis	*in vitro* (cell-based assays) *in vivo* (rat model)	[70, 74, 77]
Hesperidin	carcinogens detoxification, ↑ apoptosis, ↓tumor invasion	*in vitro* (cell-based assays)	[70, 78, 79]
Hesperetin	G1 arrest, ↓cell proliferation, ↓ metastasis	*in vitro* (cell-based assays) *in vivo* (mouse model)	[70, 80-82]
Sinensetin	G2/M arrest ,↓cell proliferation, ↑ apoptosis, angiogenesis inhibition	*in vitro* (cell-based assays) *in vivo* (zebrafish model)	[70, 83, 84]
Naringenin	↓cell proliferation, ↑ apoptosis, ↓ metastasis	*in vitro* (cell-based assays) *in vivo* (mouse model)	[70, 82, 85]

1.2.3 Fruits of *Prunus* genus

Prunus genus comprises more than 400 species of flowering shrubs and trees. Almond, peach, plum, cherry and apricot are the most economically relevant cultivars.

Plums (*Prunus domestica*), peaches (*Prunus persica*) and sweet cherries (*Prunus avium*) are botanically and compositionally similar fruits. Previous works have reported their phenolic compounds, such as flavonols, anthocyanins, catechins and hydroxycinnamates in both peel and flesh [86, 87]. Besides, bioactive terpenoides have been also detected in several varieties of these fruits including perillyl alcohol, lutein and zeaxanthin [53, 88-90].

In recent years, cherry products have been in a continue demand in the food market because of their potential positive effects on health [91]. Sweet cherries contain significant amounts of phenolic compounds such as anthocyanins, which display a wide range of health promoting benefits [92, 93]. These nutraceutical compounds are not uniformly distributed in fruit tissue. High amounts of polyphenolics and anthocyanins are observed in the fruit skin due to their functions as photoprotective agents and attractants for seed dispersal [94].

Prior researches have shown that anthocyanin members have anticancer activity [95, 96]. Antiproliferative activity in colorectal cancer cell lines was recently reported for several varieties of tart cherries [91]. Moreover, the value of cherries as fresh fruit is too high to be used for anthocyanins extraction [97]. The use of cherry wastes such as skins and pits from juice-processing industry represents a feasible alternative for these purposes.

Besides, cherries exhibit a high content of perillyl alcohol, a monoterpene molecule which has chemotherapeutic proprieties against colorectal cancer [53, 98]. Perillyl alcohol has been shown to inhibit cancer cells migration and angiogenesis, two important processes in cancer dissemination [99, 100](described in section 1.3).

Plums and peaches appear to have a wide range of health benefits, mostly due to their high content in antioxidant molecules such as neochlorogenic acid, protocatechuic acid and rutin [101-104]. Peach and plum extracts that have a high anthocyanin content can inhibit cancer proliferation and exert a differentiating effect [54]. This anthocyanins have demonstrated anti-tumorigenic effects by several mechanisms, including apoptosis induction and cell cycle arrest at G1 phase [105].

In Table 1.4 are summarized the relevant phytochemical compounds detected in cherry, plum and peach.

Table 1.4: Reported anticancer activity for cherry, plum and peach phytochemical compounds.

Phytochemicals		Mechanism of anticancer activity	Cancer model	Ref
Terpenoids	Lutein and Zeaxanthin	Carcinogens detoxification, ↑ apoptosis, angiogenesis inhibition, ↑ differentiation, ↓ ROS, modulation of immune response	*in vitro* (cell-based assays) *in vivo* (mouse and rat models)	[106]
	Perillyl alcohol	Carcinogens detoxification, ↑ differentiation, ↑ apoptosis, ↓proliferation, G1 arrest, angiogenesis and migration inhibition	*in vitro* (cell-based assays) *in vivo* (mouse and rat models)	[49, 99, 100, 107]
Phenolics	Catechin	↓Proliferation, ↑ apoptosis, ↓ ROS, angiogenesis and invasiveness inhibition	*in vitro* (cell-based assays) *in vivo* (rat model and humans)	[108, 109]
	Rutin	↓Proliferation, ↓ DNA damage, ↑ apoptosis	*in vitro* (cell-based assays) *in vivo* (mouse and rat models)	[110, 111]
	Chlorogenic and Neochlorogenic acid	↓Proliferation, invasion and migration inhibition	*in vitro* (cell-based assays)	[112, 113]
	Protocatechuic acid	Carcinogens detoxification, prevent DNA adduct formation, ↑ apoptosis , metastasis inhibition	*in vitro* (cell-based assays) *in vivo* (mouse model)	[101, 114, 115]
	Anthocyanins	G1 arrest, Carcinogens detoxification, ↑ apoptosis, ↓Proliferation, ↑ differentiation, invasion and angiogenesis inhibition	*in vitro* (cell-based assays) *in vivo* (mouse and rat models)	[105, 116, 117]

1.3 Cancer Cellular Models

Drug development process typically comprises three major steps: i) drug discovery process; ii) pre-clinical studies and iii) clinical trials (phase I, II and III). Pre-clinical studies are the stage that precedes clinical trials with is testing the drug in humans. Discovery and pre-clinical development is a continuous process resulting in preliminary pharmacology and toxicology studies [118]. In this phase the main goal is to evaluate product bioactivity, effectiveness, cytotoxicity, pharmacodynamics and pharmacokinetics. In the last two decades, several attempts have been made to develop cellular models to minimize the gap between cell-based assays and animal studies frequently used in pre-clinical phase. This allows a reducing of experimental uncertainties arising from traditional culture systems and, consequently, the cost of drug screening process [119].

Cellular models for colorectal cancer can display a unique tool to study tumors and their metastatic capacity. There are several adenocarcinoma cell lines derived from colon tumors at diverse points of differentiation and development stages. Tumor cell lines can be an important resource for understanding cancer initiation and progression. They present an identical spectrum of genetic alterations as primary tumors (described in section 1.1) [120]. In Table 1.5 is present the most common genetic alteration found in eight colon cancer cell lines.

Table 1.5: Genetic alterations and mutated genes in several colon cancer cell lines [120].

Cell line	Sex/age	*APC*	*K-ras*	*p53*	*β-catenin*	*MMR*
Lovo	M56	+	+	-	-	+
HCT116	M?	-	+	-	+	+
SW48	F82	-	-	-	+	+
HCT15	M?	+	+	+	-	+
LS1034	M54	+	-	+	-	-
HT29	F44	+	-	+	-	-
SW480	M51	+	+	+	-	-
Colo320	F55	+	+	+	-	-

During discovery phase and preclinical development of anticancer drugs, these are tested for their efficacy and potential, usually using cells grown *in vitro* on culture plates as monolayers (2D). Traditionally, 2D cell culture involves growing cells on solid, impermeable adherent surfaces. These monolayer cultures are easy and convenient to set up with high cell viability and have contributed greatly to our understanding of several diseases processes [121, 122]. However, these cellular models have many limitations and usually drugs do not work as effectively *in vivo* as in 2D model [121, 123]. Cell culture in 2D systems is a poor physiological model in comparison with *in vivo* systems, mainly due to the geometric differences between 2D culture and tissues, which are three-dimensional (3D) [124, 125]. Thus, the cells lose the capacity to respond to the molecular gradients in 2D [126]. It is, therefore, necessary to improve *in vitro* cell-based testing methods for a better perdition of drug candidate efficacy and safety [127].

The lack of stroma and structural architecture are the main limitations of 2D monolayer models. Organ cultures could provide a better model, however, it is difficult to obtain specimens and the poor viability of the tissues cultured are major obstacles [128].

1.3.1 Three Dimensional Models

3D cultures or multicellular tumor spheroids (MCTS) were first described, at the beginning of last century [129]. They were considered an improved *in vitro* model to simulate biological characteristics of tumor and consisted in 3D structures with a certain complexity [130]. The use of 3D *in vitro* systems has been recognized as a potential link to minimize the gap between monolayer cultures and animal model studies [127].

Tumor cells in spheroids show a higher degree of morphological and functional differentiation than in 2D culture [131]. One major advantage of 3D cancer models is their reproducible concentric arrangement of different cell populations which is an inherent property of solid tumors [132]. This gives a stratified composition, with proliferating cells in the outer rim, followed by a quiescent layer of cells and, eventually, necrotic cells in the spheroid center (Figure 1.9) [133]. Beyond altered gene expression and resistance to cancer treatment, the cell-cell and cell-matrix contacts in compact spheroid can also limit the diffusion of nutrients, oxygen and other compounds [125, 134]. In addition, poor efficiency of mass transport also leads to a metabolic waste accumulation inside the spheroids, like *in vivo* tumors [135].

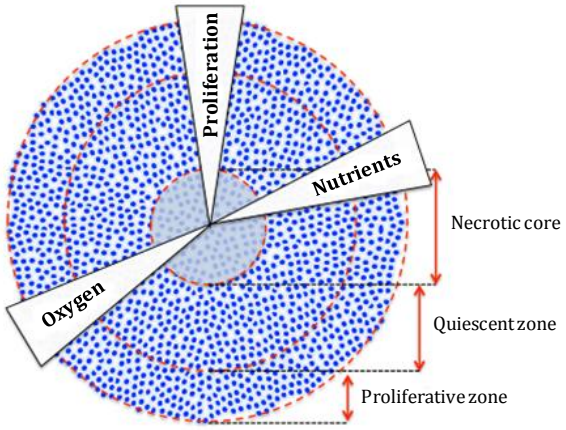

Figure 1.9: Multicellular tumor spheroid scheme. Cells are organized forming a sphere spheroid with different zones, a proliferative, quiescent and central necrotic area. Oxygen, nutrients and proliferation gradients are indicated [136].

Co-cultivation of multiple cell types is possible in 3D cultures, allowing the study of the interactions between epithelial and stromal cells, such as fibroblasts, which regulate normal and neoplastic development. The interactions and support from stromal elements and ECM plays a crucial role in tumor biology. These parameters can determine the behavior and gene expression of the cells [137]. Cell shape and tissue architecture depends on various adhesion molecules, consequently, every alteration in these molecules has relevance to cancer environment [138]. Therefore, recapitulating these *in vitro* can potentially minimize the relevance of *in vitro* models and better mimic of the *in vivo* like response to cancer therapies. The culture of colon cancer spheroids has been described since 1986 and has already been used for multiple *in vitro* studies [139-141]. However, co-cultures of colon cancer cells with cancer associated fibroblasts have been described only recently [142, 143].

The cell-cell and cell-matrix interactions in the complex 3D model not only affects drug action and penetration but it is also essential in the distribution and function of physiologically occurring factors. These biochemical effectors that play an important role in the regulatory mechanisms of cell growth, differentiation and death include hormones and growth factors. This microenvironment is important for the regulation of normal cell function and it may be useful to understand how it regulates tumorigenic phenotypes, structural and biochemically. Despite the complexities of 3D spheroids co-cultures, these models provide a strong complementary use to the animal models [137].

There are several methodologies to achieved 3D culture from cell lines, primary cells and organs, including spontaneous aggregation, liquid overlay cultures, and stirred culture systems [137]. The advantages and disadvantages for each culture systems, depending on the type of experiment and the final model. It is important to take in consideration the increased time and cost of experimental set-up and the model optimization and validation (Table 1.6) [122].

Traditionally, spheroids were obtained by spontaneous cell aggregation, generating spherical cellular conglomerates. Spheroids formed by this technique are analogous to avascular tumor nodules in terms of growth kinetic, with populations of proliferating, quiescent and necrotic cells. These different cell populations appear mostly due to mass transport limitations and also recreate the situation observed in intravascular microregions of large tumors or micrometastases prior to vascularization [144]. Other similar way to get 3D spheroids is ensuring conditions in which the adhesive forces between the cells are greater than the substrate plated on. Liquid overlay techniques (forced-floating and hanging drop methods) promotes a spontaneous aggregation, preventing cell matrix deposition. Thus, spheroids formations can even be induced in cell lines which are difficult to aggregate (Figure 1.10 (a) and (b)) [145].

Stirred culture systems present great advantages to grow 3D spheroids. These methods include gyratory rotation, rotary cultures, rotating-wall vessel bioreactor (RWV) and stirred-tank systems such as spinner flasks. In contrast to the static environment of liquid overlay cultures, which are useful to study the individual spheroid, the dynamic suspension of spinner flasks allows the production of larger numbers of spheroids. The spinner's impeller mixes and maintains the cells in suspension creating a fluid movement that is engineered to aid mass transport of nutrients to the center of spheroid (Figure 1.10 (d)). Spinner flask culture was the most widely used method for culturing large numbers of

multicellular tumor spheroids. However, other successful methods, including gyratory shakers have also been used, as well as, RWV bioreactor which maintains cells in a dynamic fluid suspension mixed by minimal hydrodynamic forces. The culture flask rotates whole on its horizontal axis, providing the mixing of the cells. The vessel is completely filled with medium minimizing fluid turbulence and shear forces with a semi-permeable membrane providing aeration and the elimination of bubbles (Figure 1.10 (c)) [146, 147].

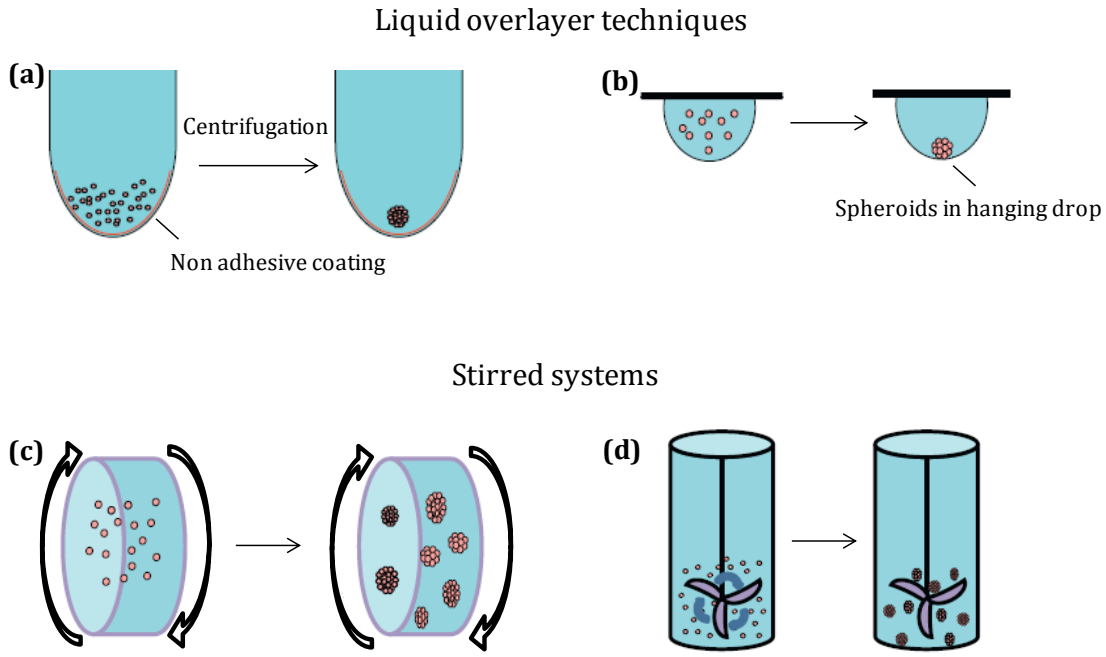

Figure 1.10: Common methods for multicellular spheroid formation: (a) forced floating, (b) hanging drop, (c) rotating-wall vessel bioreactor and using (d) spinner vessel bioreactor. (adapted from [148])

Finally, 3D cultures in environmental controlled stirred-tank bioreactors working in perfusion mode have been developed for culture and analysis of 3D tissues. These systems allow an automatic replenishment of exhausted media and control the addition of fresh medium. Further, it enables a tight regulation of extracellular environment including fluid shear and the concentration gradients of biochemical molecules. Besides the control of temperature, pH, oxygen, nutrients and metabolites, bioreactors allow the automatic feeding and effective mass transfer [149, 150].

In addition to the spheroid culture, various alternative cell culture strategies are available as tools for engineering 3D models, including the use of microcarrier beads as scaffolds. Microcarriers have provided many advantages to cell culture such as supporting the aggregation of attachment dependent cells and cell lines which do not spontaneously spheroid. Furthermore, microcarriers can be used as a platform to co-culture different cell types [137, 151]. Scaffolds are often used with the possibility of adding growth and regulatory factors. In the past decade, enhanced scaffolds have been introduced as improved support in natural molecules (collagen composite), synthetic/semi-synthetic polymers (polyethylene glycol or hydrogels) or a combination of these materials. The major advantage of these scaffolds is the great potential to recreate the natural physical and structural environment of living tissue. Has been demonstrated to promote signalling pathways that regulate migration, proliferation and differentiation [152-154] .

In Table 1.6 the main advantages and disadvantages of common 3D cell culture systems are summarized.

Table 1.6: Major advantages and disadvantages of common 3D culture methods.

Culture system	Advantages	Disadvantages
Static systems	• Relatively simple • Inexpensive • Suitable for high-throughout • Spheroids production are easily accessible	• Labor intensive • Small culture volumes difficult medium exchange without disturbing cells • No control over size of spheroid
Stirred systems	• Simple to culture • Large-scale production easily achievable • Better nutrient transport • Spheroids production are easily accessible	• Specialized equipment required • No control over size of spheroid • Cells are exposed to shear stress forces in spinner flasks (problematic to sensitive cells)

1.4 Thesis Goal

The major goal of this thesis is the evaluation of the anticancer effect of phytochemical extracts, using 3D cellular model of colon cancer. For this propose a 3D model using HT29 cells growing as spheroids was developed and characterized.

The work was divided in three major parts as schematically presented in Figure 1.11.

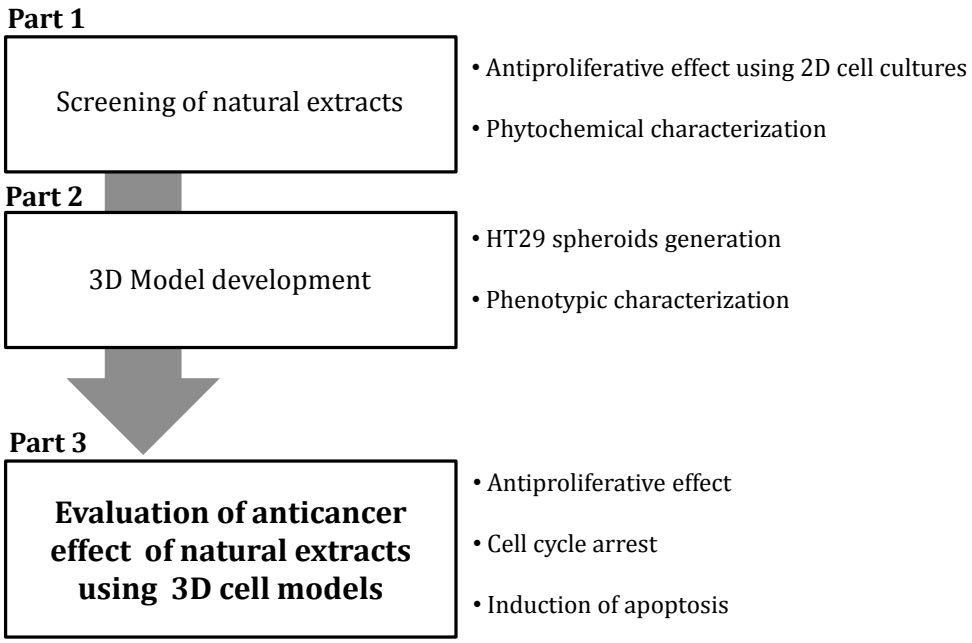

Figure 1.11: Structure of the thesis.

In the first part, the antiproliferative effect of natural extracts obtained from cherries, peaches, plums, oranges and olive seeds were tested in 2D monolayer cultures. 2D dose-response curves were performed to determine the effective dose value (EC50) of each extract. In this part, phytochemical characterization of the extracts was also carried out.

The second part was focused in the development of 3D cell model of colon cancer using dynamic stirred culture system. Tumor spheroids were grown in spinner flasks and several culture parameters were optimized. Phenotypic assessment was also performed in order to better characterize the 3D cell model.

In the third part of the work, chemotherapeutic potential of the most promising phytochemical-rich extracts were evaluated using 3D model of colon cancer and results were compared with 2D monolayer results.

2 Experimental Procedure

2.1 Natural extracts

Olive seeds extracts from six olive trees varieties (*Cobrançosa, Zambujeiro, Picual, Arbosana, Koroneiki* and *Arbequina*) were performed by conventional solvent extraction (CSE) in the context of an ongoing project [155].

Initially, the seeds were obtained by breaking the olive stones. The solid-liquid extraction was carried out using 2 g of each seed sample and 10 ml of solvent mixture containing EtOH:H_2O (80:20,v/v). Samples were mixed by vortex during 5 minutes and then centrifuged for 15 min at 5000 rpm. The extraction procedure was repeated once again and finally supernatant was filtered and concentrated by rotary evaporator. Samples were dissolved in EtOH:H_2O (80:20,v/v) and stored at -20 ^{0}C after being filtered through a 0.45 µm filter Acrodisc® (Pall, USA).

Extracts of cherry, plum, peach and orange residues were performed by Nutraceuticals and Delivery group of IBET (Oeiras, Portugal) using high pressure technology. All of the raw-materials used for extraction are residues of fruit juice production (peels, seeds and core), or crop residue (cherry culls). The extracts were obtained under variable extractions conditions and using diverse CO_2/EtOH ratios.

In Table 2.1 are summarized the extraction conditions used to obtain high pressure natural extracts.

Table 2.1 : Extraction conditions used to obtain fruit residues extracts with high pressure technology.

Extract	**CO_2 pre treatment**	**Pressure (MPa)**	**Temperature (K)**	**Time (min)**	**% CO_2/EtOH**	**Ref**
Orange peel	-	25	323	30; 60; 90;120	80/20	[156]
Cherries	60 min	25	323	30	90/10	[90]
Peach	60 min	25	323	30	90/10	[90]
Plum	60 min	25	323	30	90/10	[90]

2.2 Phytochemical characterization

2.2.1 Terpenes analysis by thin layer chromatography (TLC)

The detection of terpenes, such as perillyl alcohol and linalool, was performed by thin layer chromatography (TLC).

TLC analysis was carried using silica gel plates with a 254 nm fluorescent indicator with aluminum base (20 cm x 20 cm) (Macherey-Nagel, Duren, Germany). Dichoromethane was used as mobil phase and for detection a mixture of 1% ethanolic vanillin + 10% ethanolic sulphuric acid + Burchard reagent (1% acetic anhydride and 1% suphuric acid ethanolic) was applied. At the end of elution, the plate was sprayed with prepared solutions and heated at 110 ^{0}C for 10 minutes. Then, the plate was revealed with Burchard reagent and the visualization was performed under 254 nm UV light.

2.2.2 Phenolic analysis by high performance liquid chromatography (HPLC)

The phenolic HPLC analysis of natural extracts was performed by Analytical Group of IBET (Oeiras, Portugal) coordinated by Dr. Rosário Bronze. Briefly the analysis was carried out using a Surveyor apparatus form Thermo Finnigan with a diode array detector (Thermo Finnigan-Surveyor, San Jose, CA, USA) and an electrochemical detector (Dionex, ED40) [157]. Separations were performed at 35 ^{0}C in a LiChrospher C18 (5 µm, 250 mm x 4 mm i.d.) column from Merck with a guard column of the same type. The samples injection was carried out using a 20 µl loop. The gradient mobile phase consisted of eluent A (phosphoric acid (0.1%)) and eluent B (phosphoric acid (0.1%)-acetonitrile-water 1:900:99, v/v/v) at a flow rate of 700 µl/min. The following eluents gradient was used: 0.10-25 min from 0 until 8.9% eluent B; 25-70 min, from 8.9 until 31.1% eluent B; 70-75 min, with 31.1% eluent B; 75-85 min from 31.1 until 44.4% eluent B; 85-90 min, with 44.4% eluent B; 90-125 min from 44.4 until 90% eluent B; 125-130 min, with 90% eluent B; 130-131 min from 90 until 100% eluent B; 131-145 min, with 100% eluent B. Diode array detection was performed between 192 and 798 nm. The data acquisition system used was the Chromquest version 4.0 (Thermo Finnigan-Surveyor, San Jose, CA, USA). Chromatograms recorded at 280 nm were used to analyze total phenolics. Identification of compounds was done by comparing retention time and spectra with known amounts of pure standards (ferulic acid, vanillin and naringenin). Total polyphenol content of samples was determined using total peak area recorded at 280nm and a calibration curve with gallic acid (10-100 mg/L). Final results were expressed as gallic acid equivalents per liter of extract.

2.3 Cell-based assays

2.3.1 Cell lines and culture

Human colon cancer cell lines, HT29 and Caco2 were provided by American type Culture Collection (ATCC, USA) and Deutsche Sammlung von Microorganismen und Zellkulturen (DSMZ, Germany), respectively. Both cell lines were cultured in RPMI 1640 medium supplemented with 10% heat-inactivated fetal bovine serum (FBS) and 2 mM of glutamine. Cells were kept at 37 ^{0}C in a humidified incubator with 5% CO_2 and routinely grown in 75 or 175 cm^2 culture flasks. Cell culture medium and supplements were obtained from Invitrogene (Gibco, Invitrogene Corporation, Paisley, UK). The cell lines were split once or twice a week, the morphology and growth of cells were monitored daily.

2.3.2 Antiproliferative assay using 2D cell culture system

Antiproliferative assays were performed on human colon adenocarcionoma cell line (HT29) growth as monolayer.

The assay was carried out in 96-well microplates as described by Serra et al. [53]. Briefly cells were seeded at a cellular density of $1x10^4$ cell/well. After 24 hours of incubation in 5% CO_2 humidified atmosphere at 37 ^{0}C the medium was removed and cells were incubated with natural extracts diluted in RPMI medium supplemented with 0.5% FBS. After 24 hours, the medium was removed and cell viability was assessed using commercial PrestoBlue® Viability Reagent (Molecular Probes, Invitrogen, US). Briefly, PrestoBlue® regent (diluted 1:10) was added to each well and the microplate was incubated for 2 hours. Finally the fluoresce was quantified on a microplate fluorescent reader (FL800, Bioteck Instruments, USA) with filter appropriate for 580 nm excitation and 595 nm emission maxima. The results were expressed as a percentage of cell viability relative to the control (cells incubated with culture medium only, without natural extracts). The experiment was performed in triplicate. EC50 values (the concentration of sample necessary to decrease 50% of cell viability) were obtained from dose-response curves using software GraphPad Prism (GraphPad Software, Inc., La Jolla, CA) fit.

2.3.3 Cytotoxicity assay

In vitro cytotoxicity assays were accomplished using confluent Caco2 cells. Despite were obtained from a human colon adenocarcionoma, this cells can be used as an intestinal barrier model when cultured under special conditions. When Caco2 becomes differentiated and polarized, it shows a resemblance morphological and functional to enterocytes from small intestine. Their differentiation occurs spontaneously when cells grow in monolayer in a long term culture [158].

Cells are seeded into 96-well culture plates at a density of $2x10^4$ cell/well, and were allowed to grow for 8 days, with medium exchange every 48 hours. Extract samples, previously diluted in culture medium (RPMI with 0.5% FBS and 2mM glutamine), were added to all wells except to the control samples. Incubation with natural extracts was carried out during 24 hours and cytotoxicity evaluation was performed with PrestoBlue® Viability Reagent (Molecular Probes, Invitrogen, US). PrestoBlue® regent (diluted 1:10) was added to each well and the microplate was incubated for 2 hours. Finally the fluorescence was quantified on a microplate fluorescent reader (FL800, Bioteck Instruments, USA) with filter appropriate for 580 nm excitation and 595 nm emission maxima. Viability, expressed as percentage of living cells, was determinate relatively to the control. IC50 values were calculated from dose-response curves using software GraphPad Prism (GraphPad Software, Inc., La Jolla, CA) fit.

2.3.4 Cell culture and spheroids formation

Cells grown as a monolayer were detached with trypsin/EDTA and a density of $2.5x10^5$ cell/ml was placed into the 125 ml spinner flasks (Proculture, Corning, NY, USA). To prevent the walls attachment, spinner flasks were pre-coated with 2-3 ml of dimethyldichlorosilane (Merck 8.03452, Germany). The spinner flasks were placed on a magnetic stirrer and were maintained in culture for 12 days. Initially, a stirring rate of 40 rpm with only 60% of total volume (75 ml) was used until 8 hours after inoculation, aiming at promoting spheroids formation. To control the size of the spheroids, the stirring rates were gradually increased for 45, 50, 55 and finally 60 rpm at 8, 10, 24 and 28 hours post-inoculation, respectively. After that, aggregation kinetic was daily monitored until day 7 of culture. At day 3, the first medium exchange was performed (50% of spinner flask culture medium was replaced by fresh medium). This was a daily procedure. The culture was monitored counting nuclei, viable cells and measuring spheroids diameter.

2.3.5 Cell viability and total cell count

Total cell number assessment on culture is indispensable to evaluate the aggregation process and it is useful to draw conclusions about the dissociation method. In order to determine the total cell number present in the culture, their nuclei were counted using crystal violet method that stains nuclei in purple. Cells were previously lysed by adding lysis buffer (1% Triton X-100 in 0.1 M citric acid), at least 15 minutes, at 37 ^{0}C. Nuclei were stained in 0.1% of crystal violet.

To assess cell viability, the spheroids were centrifuged during 5 minutes at 200x g followed by washing with PBS and dissociation by adding trypsin-EDTA 0.05%. 4 minutes later, cells were resuspended in culture media (RPMI 1640 with 10% of FBS), in order to inactivate trypsin, diluted and stained with trypan blue 0.1% (Gibco, Invitrogene Corporation, Paisley,

UK). Cells with damaged membrane (non viable) are stained by trypan blue, while viable cells are not stained and therefore appear bright. Cell viability and nuclei count were performed using a hemacytometer.

In addition, spheroids viability was qualitatively assessed using fluorescent dyes, FDA and PI, to stain viable and non viable cells. Fluorescein diacetate (FDA) is a cell viability probe that measures esterase enzymatic activity, which activate its fluorescence, and cell membrane integrity, allowing intracellular retention of their fluorescent product. This dye exhibits a green fluorescence that stains viable cells. PI is a nuclear red-fluorescent molecule which is membrane impermeant excluded from viable cells. This probe only stains nucleus of membrane-compromised cells and intercalate into its double-stranded nucleic acids. Spheroids were stained with both FDA and PI, diluted 1:1000 and analyzed using fluorescence microscope (Leica DM6000). Thus, viable cells present green fluorescence and non viable red fluorescence.

2.3.6 Analysis of spheroids size and shape

During the spheroids formation process, a regular monitoring is required in order to determine spheroids size.

Using fluorescein diacetate and propidium iodide it was possible to observe viable and non-viable cells, as previously described. Colonospheres were also observed by bright field microscopy (Leica DM6000). Their average diameter was determined using ImageJ software. Ferret diameter was calculated for each spheroid with more than 50 µm diameter.

2.3.7 Flow cytometry immunophenotyping

Aiming to identify the stem cell-like character of 3D model, the quantification of $CD44^+$ cells was carried out. Antibody anti-CD44 was used to detect cells that contain expression of CD44 antigen. The quantification of cell population was performed using the fluorochrome R-Phycoerythrin (PE), which is coupled with the antibody.

Briefly, spheroids were harvested ($5x10^5$ cell) and detached as described previously (section 2.3.5). Single cells were sedimented by centrifugation at 500x g (Mikro 220R, Hettich, Tuttlingen, Germany) for 5 minutes followed by washing with 500 µl of cold FACS buffer (PBS supplemented with 1% FBS) and incubation with antibody anti-CD44-PE (eBioscience) diluted 1:20 (0.1 µg/$0.5x10^6$ cell) in FACS buffer for 1 hour at 4 ^{0}C. Isotype control was used in the same proportion to evaluate the existence of unspecific bindings. After the incubation time, cells were washed twice again with 500 µl of cold FACS buffer. The pellet was resuspended in 2 ml of FACS buffer and storage at 4 ^{0}C until the measurement in flow cytometer. Results were acquired in CyFlow space instrument (Partec, Germany). The parameters in the flow cytometer were adjusted with the corresponding isotype control antibody (IgG2b) conjugated with PE, serving as a negative control, and it

was acquired a total of 15000 events per sample in order to identify the expression of CD44 surface marker.

2.3.8 Immunofluorescence microscopy

Tumor spheroids were collected from the suspension culture and immediately fixed in 4% (w/v) paraformaldehyde (PFA) and 4% (w/v) sucrose solution in PBS for 30 minutes. After 2 washes with PBS, spheroids were dehydrated in PBS solution with 30% of sucrose. For the cryosectioning, colonospheres were frozen at -80 C in Tissue Teck OCT™ (Sakura) and were sectioned in cryostat (Leica) in sections of 10 μm.

For 2D controls HT29 cells were cultured as monolayer in glass coverslips, inoculated at $1x10^4$ cell/well. After 24 hours of seeding, cells were gently washed with PBS and fixed with 4% (w/v) PFA solution in PBS with 4% (w/v) sucrose for 20 minutes.

Cryosections and 2D controls were initially washed twice with PBS followed by permeabilization with 0.1% Tx-100 solution in PBS for 10 minutes. At the end of permeabilization step, cells were washed 2 times with PBS and blocked with 0.2% of FSG in PBS for 30 minutes. Primary antibody was diluted in 0.2% FSG solution and it was added to the cells and they were incubated during 2 hours. After 2 washes with PBS, cells were incubated for 1 hour with secondary antibody in 0.2% FSG solution. The list of primary and secondary antibodies is presented in Table 2.2. Cryosections were finally washed twice with PBS, mounted in ProLong mounting medium contain DAPI (Invitrogen) and visualized using a fluoresce microscope (Leica DM6000, Germany). Besides the antibodies, it was also used Alexa Fluor® 488 Phalloidin (invitrogen) diluted 1:100, a bicyclic peptide, which binds F-actin with high selectivity and presents green fluorescence due to the presence of Alexa Fluor® 488.

Table 2.2 : List of antibodies and respective dilutions used for immunofluorescence microscopy assays

Antibody	Marker	Concentration	Manufacturer
Anti-vimentin	Mesenchymal cells	1:200	Sigma
Anti-Cytokeratin 18-FITC	Epithelial cells	1:100	Sigma
Anti-E-Cadherin	Epithelial cells	1:300	BD
Anti-β-Catenin	Cytoplasmatic/nuclear localization - EMT	1:200	Santa Cruz Biotechnology
Anti-CD44-PE	Cancer stem cells	1:50	eBioscience
M30 cytoDEATH	Early apoptosis	1:30	Roche
Anti-mouse Alexa Fluor 488	(secondary antibody)	1:500	Invitrogen
Anti-rabbit Alexa Fluor 594	(secondary antibody)	1:500	Invitrogen

2.3.9 Antiproliferative assay using 3D culture systems

Before the evaluation of antiproliferative effect of natural extracts on colonospheres several viability assays were studied, such as, CellTiter 96® Aqueous One and PrestoBlue®. To assess reagent diffusion and the range of linearity of each method, standard curves were tested using different spheroids densities and sizes. The spheroids were diluted in culture media (RPMI with 10% FBS and 2mM glutamine) and placed in 96-well plate pre-coated with Poly-L-Lysine (10 µg/ml) followed by the addition of respective viability reagent (see appendix A). These methods were applied for three spheroid sizes, 300, 400 and 500 µm of diameter.

Antiproliferative assays were performed using natural extracts and HT29 spheroids with 300, 400 and 500 µm of diameter that were cultured in spinner flasks during 3, 5 and 7 days.

Cell spheroids were seeded at a density of approximately 4 spheroid/well, in 96-well microplates pre-coated with Poly-L-Lysine (10 µg/ml). Cell viability was assessed using PrestoBlue® reagent. This measurement was essential to estimate the number of cell in each well. Briefly, 10 µl of PrestoBlue® was added to each well. After an incubation period of 2 hours, well plate was centrifuged (SIGMA 3K15, Sigma Laborzentrifugen, Germany) for 4 minutes at 200x g and supernatant was placed into a black-96-well microplate to measure fluorescence intensity. Orange peel (fraction 30 min) and Brooks cherry extracts, previously

diluted in RPMI culture medium supplemented with 0.5% FBS, were added to each well and incubated for 24 or 72 hours. After that, extracts were removed and PrestoBlue® diluted in culture media was added according supplier protocol. PrestoBlue® viability reagent fluoresce was measured by microplate fluorescence reader (FL800, Bioteck Instruments, USA) at an excitation and emission wavelengths of 580 and 595 nm, respectively.

The assay was made using 6 replicates of each extract concentration and results were expressed in terms of percentage of growth inhibition, in relation with control (colonospheres without extract incubation). Cell viability was calculated using following equations:

$$\%\ cell\ viability = \frac{FI\ ratio\ (trated\ cell)}{FI\ ratio\ (average\ of\ control\ cells)} * 100$$

$$FI\ ratio = \frac{FI_{24/72}}{FI_0}$$

Where FI_0 is the fluorescence intensity of cells before incubation with extract and $FI_{24/72}$ is fluorescence intensity of cells after 24 or 72 hours of extract incubation.

All EC50 were calculated from dose-response curves using software GraphPad Prism (GraphPad Software, Inc., La Jolla, CA) fit.

2.3.10 Apoptotic activity

The assessment of cells apoptotic activity can provide important complementary information about drug's chemotherapeutic effectiveness.

Apoptotic activity of natural extracts on colonspheres was performed with NucView™ 488, caspase-3 substrate, and MitoView™ 633, red-fluorescent mitochondrial dye. Caspase-3 substrate, which is non-fluorescent and non DNA dye, penetrates on cell membrane and it is cleaved by caspase-3/7 in cytoplasm, forming a high-affinity DNA dye. This DNA probe migrates to cell nucleus originating bright green stain. Besides, NucView™ 488 is able to stain cell nuclei, which undergo morphological changes during apoptosis. Consequently, apoptotic cells display a lower red fluorescence signal and higher green fluorescence when compared with non-apoptotic cells.

In this experiment tumor spheroids were placed in a 24 well-plate at a density of 100 spheroids/well and Orange peel (0.5 mg extract/ml) and Brooks cherry (0.1 mg extract/ ml) extracts were added. Cells were kept during 24 hours in a humidified atmosphere at 37ºC with 5% CO_2. At the end of the exposure period, supernatant was removed followed by the addition of 200 µl of fresh culture medium containing 1µl of each dye (NucView™ 488 and MitoView™ 633). During 2 hours, cells were stained with fluorescent dyes. The plate was centrifuged (SIGMA 3K15, Sigma Laborzentrifugen, Germany) for 5 minutes at 200x g and cells were washed with PBS. Spheroids were resuspended in PBS (200 µl) and observed in fluorescence microscope (Leica DM6000, Germany) and in spinning-disc confocal microscope (Nikon Eclipse Ti-E, Japan).

2.3.11 Cell cycle assessment

Using flow cytometry is possible to distinguish cells in different phases of the cell cycle. By fluorescence labeling of cell's nuclei in a suspension, it is possible to correlate fluorescence intensity with the amount of DNA that they contain. Cells in G1 phase will have one copy of DNA, consequently they will have the half of fluorescence intensity when compared with cells in phase G2/M, which contain two copies of DNA. Since the cells in phase S are synthesizing DNA, they present intermediate fluorescence intensity.

Cell cycle analysis was performed by fluorescence-activated cell sorter (FACS) using propidium iodide (PI) as a dye. Briefly, 1 ml of spheroids suspension containing approximately 100 colonospheres was collected from spinner at day 7 of culture and placed in a 12-well plate. During 24 hours, all the cells were incubated with orange peel (fraction 30 min) and Brooks cherry extracts (0.63 mg extract/ml for orange and 0.18 mg extract/ml for cherry), except control cells that were incubated with culture medium, alone or culture medium plus solvent. After that, spheroids were transferred to centrifuge tubes and centrifuged at 200x g during 5 minutes. The supernatant was removed and the pellet was washed with PBS. Spheroids were then dissociated with 200 µl of trypsin/EDTA 0.05% for 3 minutes followed by addition of 800 µl of RPMI medium (10% FBS) for an efficient trypsin inactivation. Cells were centrifuged at 200g for 10 minutes. After that supernatant was removed, cells were washed with cold PBS and centrifuged again (200x g, 10 min). Cells, at a density of $1x10^6$, were incubated with 1 ml of a solution containing PI (50 mg/ml), Triton-x 10x (1.5%), ribonuclease A (0,7 U/ml) and NaCl (0.01M) overnight at 4 ^{0}C. Analysis was carried out using a flow cytometer (CyFlow Space, Partec, Germany) and cell cycle analysis was done using software FlowMax cell cycle platform (Partec, Germany).

3 Results and Discussion

Recently, special interest has been focused on the recovery of wastes in an effort to find value added applications to these residues. In this thesis, natural extracts produced by clean extraction technologies from waste residues of fruit processing industry/ crops were evaluated in terms of their potential chemotherapeutic effect using 2D and further 3D cell models of human colorectal cancer cell line HT29.

3.1 Screening of the antiproliferative effect of natural extracts

In this work, several natural extracts obtained by different extraction methods as well as different extraction conditions, were screened for their antiproliferative effect. The selection of samples was based on previous studies related with the anticancer potential of raw material and the efficacy of extraction technologies to isolate the bioactive molecules.

3.1.1 Olive seed extracts

Initially, olive seed extracts, obtained by conventional solvent extraction (80:20 etanol:water v/v) from six varieties, namely *Cobrançosa, Arbequina, Arbosana, Koroneiki, Picual* and *Zambujeiro* were explored as potential sources of bioactive molecules. Figure 3.1 presents the phenolic profiles of all samples obtained by HPLC-DAD.

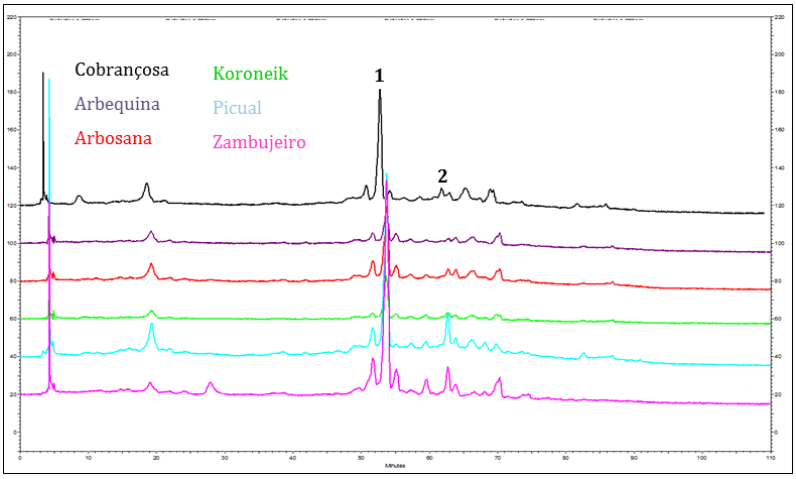

Figure 3.1 : Phenolic profiles of CSE extracts of olive seeds obtained by HPLC-DAD recorded at 280 nm. Legend: 1- nuzhenide; 2- oleuropein.

Results showed that phenolic profiles of different olive seed varieties were very similar, however, some variations in peaks intensity were observed. Nuzhenide and oleuropein that were previously identified in olive seed composition, were the main phenolic compounds identified in all extracts [62].

Nuzhenide content of all samples, as well as total phenolic concentration, was also determined by HPLC and results are presented in Table 3.1.

Table 3.1 : Phytochemical characterization of olive extracts.

CSE extract	TPC * (mg GAE/L extract)	Nuzhenide ** (mg OE/L)
Cobrançosa	76.98	94.77
Arbequina	23.77	29.00
Arbosana	42.25	62.14
Koroneiki	17.94	44.07
Picual	75.94	151.65
Zambujeiro	39.84	173.99

* Total phenolic content (TPC) was determined using total phenolic peaks area and gallic acid standard curve. The results are expressed in mg of gallic acid equivalents/L of extract.
** Nuzhenide content was determined using total nuzhenide peak area using oleuropein standard curve. The results were expressed in mg of oleuropein equivalents/L of extract.

Among all extracts, *Cobrançosa* and *Picual* displayed the highest phenolic amount, whereas *Koroneiki* presented the lowest concentration in phenolic compounds. *Zambujeiro* extract was the one that presented the highest concentration of nuzhenide.

The antiproliferative effect of all samples was evaluated in HT29 cells and results showed that only *Zambujeiro* extract was able to inhibit HT29 cells growth (Figure 3.2).

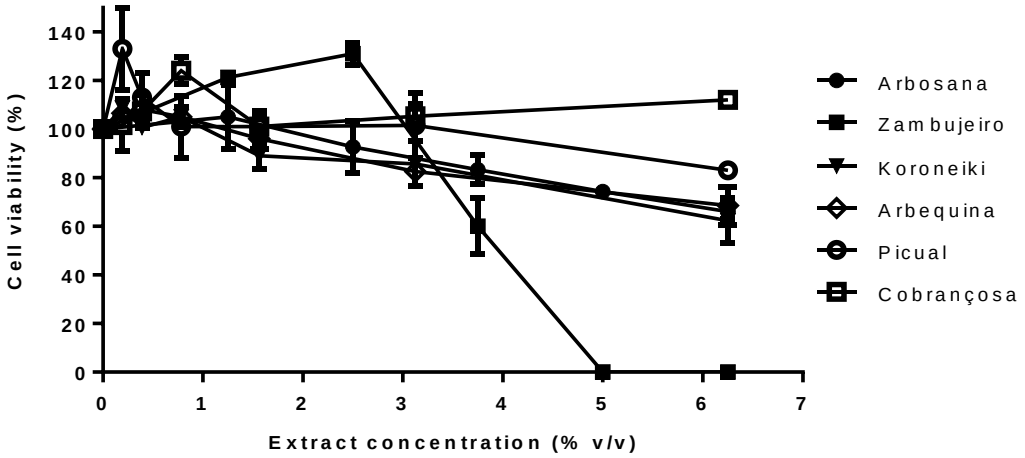

Figure 3.2: Antiproliferative effect of extracts from olive seeds varieties on human colon cancer cells HT29 (incubation time:24 h; Data are means ± SD (n=3)).

For this sample, the effective dose value (EC50) was 4.084 (% v/v). It is important to highlight that this extract was not cytotoxic in Caco2 cells, which are a good model of intestinal barrier.

When compared with phytochemical characterization of the extracts, it could be suggested that the higher antiproliferative response could be related with the presence of high nuzhenide content. Nuzhenide is a phenolic compound commonly present in this type of natural sources, but, up to now, there is no information about health benefits.

Further studies should be performed in order to identify the main bioactive compounds of *Zambujeiro* extract. Moreover, since the EC50 value is relatively high, other extraction techniques should be explored to isolate the main bioactive compounds responsible for the anticancer effect.

3.1.2 Fruit residues extracts

Natural extracts from orange peel, plum, peach and cherries waste residues were performed by high pressure technology. It is important to note that this technology allows an easier and more selective extraction of phytochemical compounds from natural sources than others conventional methods [155].

Orange juice industry waste residues, namely orange peel, present a flavonoid-rich composition that are already reported to exhibit high anticancer effect [70]. In this work, orange peel extracts produced by high pressure extraction using pressure, temperature and co-solvent conditions already reported to efficiently isolate PMFs, were evaluated for their antiproliferative effect (Table 2.1) [156]. Samples were obtained at different extraction times in order to select the most effective fraction to inhibit proliferation of HT29 cancer cells.

Orange peel extracts collected after 30, 60, 90 and 120 minutes of extraction were characterized in terms of phenolic profile. Figure 3.3 shows the phenolic content of all factions.

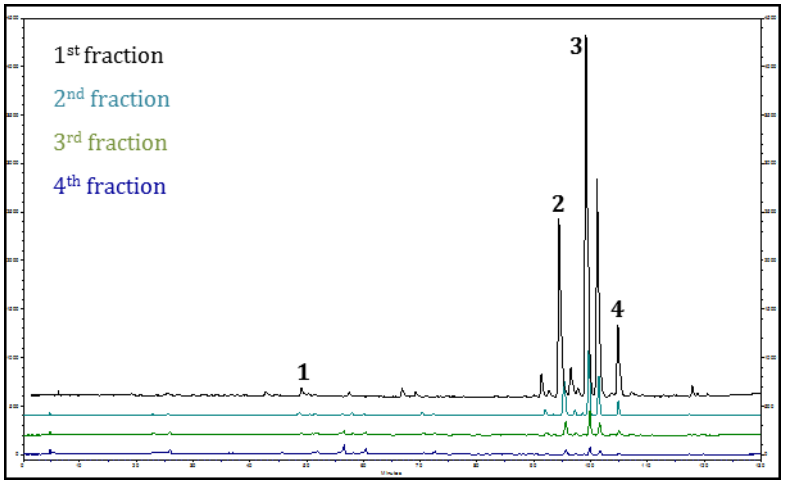

Figure 3.3: Phenolic profiles of all orange peel fractions. The results were obtained by HPLC-DAD-UV recorded at 280 nm. Legend: 1- ferulic acid; 2- sinensetin; 3- nobiletin; 4- tangeretin

Phenolic profiles of all orange peel extracts were similar, although the fraction collected in the first 30 minutes of extraction (1st fraction) presented the highest peaks intensity.

In order to complement this phytochemical characterization, the total phenolic content was determined (Table 3.2). These results confirm the high phenolic content of the first extract fraction (30 minutes).

Table 3.2: Total phenolic content of orange peel extracts

Orange Peel extracts	TPC* (mg GAE/L extract)
1st fraction (30 min)	2205.9
2nd fraction (60 min)	451.84
3rd fraction (90 min)	226.13
4th fraction (120 min)	225.76

* Total phenolic content (TPC) was determined using total phenolic peaks area using gallic acid standard curve. The results are expressed in mg of gallic acid equivalents/L of extract.

In fact, the first fraction had 5 to 10 times more phenolic content than the other orange fractions (Table 3.2).

The antiproliferative effect was also evaluated and the extract collected in the first 30 minutes of extraction displayed the highest anticancer activity with an effective dose value of 0.488 ± 0.031 mg extract/ml (Figure 3.4).

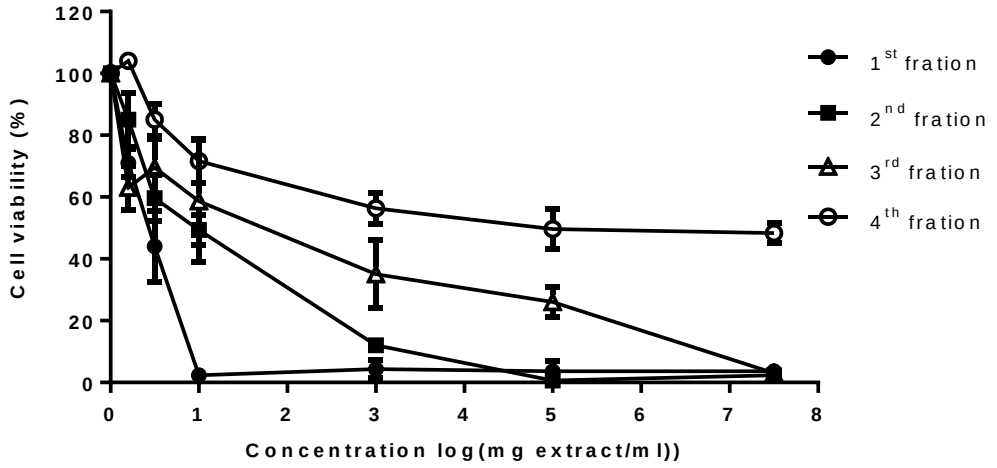

Figure 3.4: Antiproliferative effect after 24 hours of incubation with orange peel fractions collected at different extraction times on HT29 cell line. Results were mean ± SD (n=3).

Results presented in Figure 3.4 also showed that the antiproliferative effect of extract samples decreased with the extraction time, indicating that the main bioactive compounds were selectively extracted during the first 30 minutes of process. These findings are in accordance with the phytochemical composition, in particular, PMFs content of orange extracts. Sinensetin, nobiletin and tangeretin were some PMFs detected in high concentration in the 1st fraction of orange peel extract. These compounds are already reported to exhibit antiproliferative effect on gastric and colon cancer cell lines [70, 83]. Additionally, PMFs present low polarity and planar structure. These features enhance their biological activity due to the high membrane permeability and binding proprieties [70].

In the case of cherries, the extracts were obtained using a fractioned high pressure extraction process previously optimized to isolate perillyl alcohol-rich fractions from this type of raw material [53]. Cherry extracts used in this work were derived from two different cherry varieties, Brooks and Sweet Heart. Since plums and peaches belong to the same

genus (*Prunus*) of cherries, they also present similar composition. Therefore, extracts derived from plum and peach residues were performed using the same extraction process and were also tested in this study.

Terpenes composition of plum, peach and cherry extracts (Sweet Heart and Brooks extracts), was evaluated by TLC (see appendix B). The methodology allowed the detection of perillyl alcohol in all the analyzed extracts.

The phenolic profiles were analyzed by HPLC-DAD and the main compounds identified include vanillin and naringenin in peach extract and sakuranin in both cherry extracts (Figure 3.5).

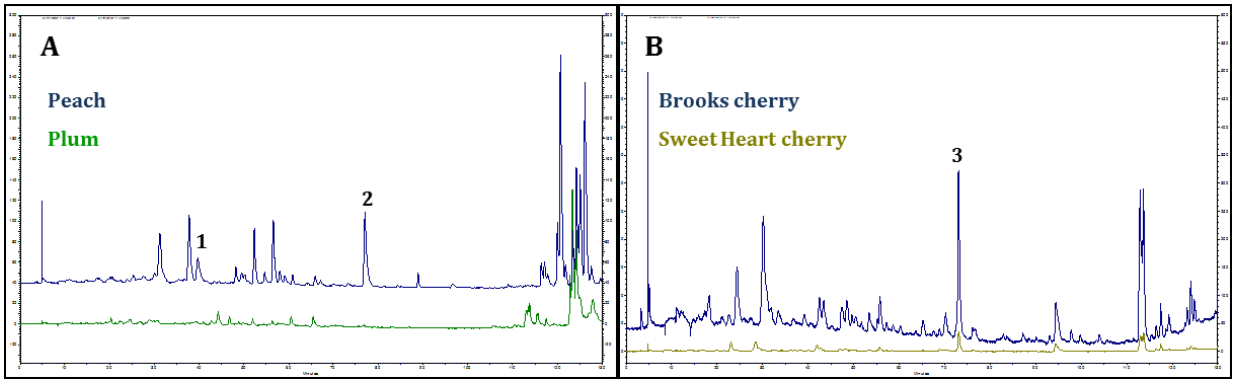

Figure 3.5: Phenolic profiles of plum and peach (A) and both cherry extracts (B). The results were obtained by HPLC-DAD-UV recorded at 280 nm. Legend: 1- vanillin; 2- naringenin; 3- sakuranin.

Aiming at comparing all extracts, the total phenolic content was assessed by HPLC and the results are presented in Table 3.3.

Table 3.3: Phenolic characterization of *Prunus* extracts

***Prunus* extract**	**TPC* (mg GAE/L extract)**
Sweet Heart cherry	74.0
Brooks cherry	1049.9
Plum	118.5
Peach	308.0

* Total phenolic content (TPC) was determined using total phenolic peaks area using gallic acid standard curve. The results are expressed in mg of gallic acid equivalents/L of extract.

Among all extracts, Brooks cherry exhibited the highest phenolic content whereas Sweet Heart cherry extract presented the lowest value. This difference between phenolic content of cherry extracts was also revealed in Figure 3.5 which was evident for the highest peaks intensity of Brooks cherry sample.

Antiproliferative activity of cherries extracts, using Sweet Heart and Brooks varieties, are presented in Figure 3.6.

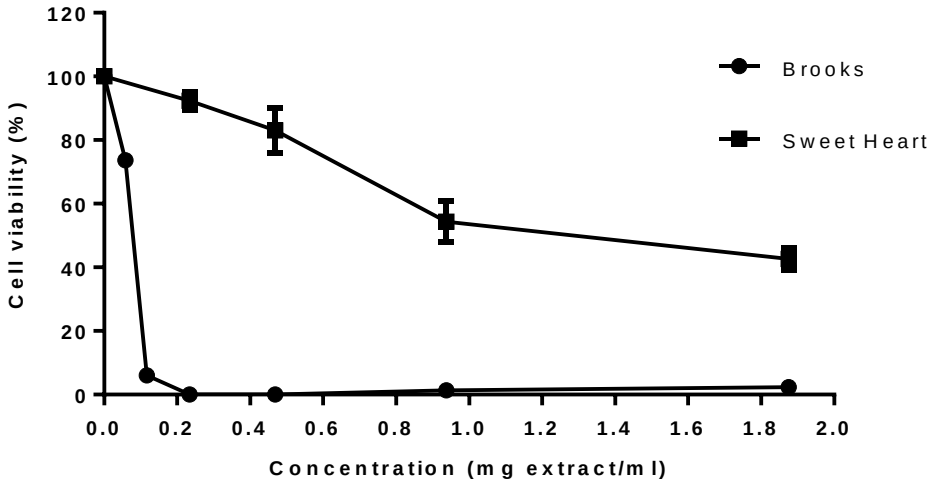

Figure 3.6 : Antiproliferative activity of Brooks and Sweet Heart cherry extracts in HT29 colon cancer cell line (incubation time=24 h; results are mean ± SD (n=3)).

Between the two cherry extracts, Brooks cherry was the most effective in inhibiting HT29 cells proliferation. The required amount of extract to decrease cancer cell viability was extremely low (EC50=0.092 ± 0.014 mg extract/ml). This result suggests that extraction of this fruit variety was highly selective to isolate of powerful anticancer agents. The high antiproliferative effect of Brooks cherry could be related not only with the presence of perillyl alcohol, compound already described to be a powerful anticancer agent, but also with the highest phenolic content of this sample (Table 3.3).

The antiproliferative effect of plum and peach extracts is presented in Figure 3.7.

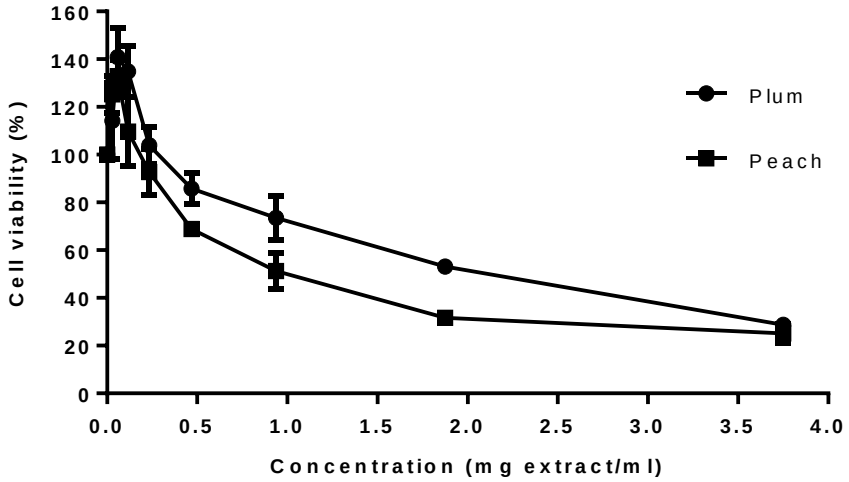

Figure 3.7: Antiproliferative effect of plum and peach extracts on HT29 cells (incubation time=24 h; results are mean ± SD (n=3))

Results showed that dose-response curves of plum and peach residue extracts were similar. Between the two samples, peach extract showed lower EC50 value (1.217 ± 0.275 mg extract/ml) than plum extract (EC50=2.767 ± 0.666 mg extract/ml). The higher anticancer effectiveness of peach sample could be related to the presence of a higher content in phenolic compounds (Figure 3.5 (A)). As presented in Table 3.3, this extract exhibited three times more total phenolic content than plum extract. As mentioned above, vanillin and naringenin were the main compounds identified in peach samples. This compounds were already reported to have potent antiproliferative activity and pro-apoptotic effect on HT29 cancer cell lines, and, therefore, could be the main responsible of the higher antiproliferative effect of peach extract [159, 160].

In Table 3.4 are summarized the EC50 values obtained for all screened extracts.

Table 3.4: EC50 values of natural extracts (incubation time=24 h).

Phytochemical extract	**EC50 (mg extract/ml)**
Orange peel (1st fraction)	0.488 ± 0.031
Brooks Cherry	0.092 ± 0.014
Sweet Heart Cherry	1.608 ± 0.416
Peach	1.217 ± 0.275
Plum	2.767 ± 0.666

Among all samples, Brooks cherry and orange peel extracts showed the lowest effective dose values, and thus were the most promising natural extracts to be further tested in more robust cancer cell models.

It is important to mention that for all samples, EC50 doses were not cytotoxic in Caco2 cell model.

3.2 3D model Development

3.2.1 Generation of 3D model of colon cancer

In recent years, several authors have been developing colon cancer 3D models, including the use of HT29 cell line, however, the majority of these models are based on static culture systems [161-163]. These cultures present several limitations such as the low spheroid numbers generated and the selection of the most aggregative cells, as these are systems based on spontaneous cell aggregation. The use of stirred systems for the 3D culture of cancer models presents several advantages that might overcome some of the limitations associated with static 3D culture systems. With the goal of developing a robust and reproducible 3D colon cancer model of HT29 cells, a stirred system was used.

Spheroids formation and growth was carried out using spinner-vessels Corning® Proculture® spinner flasks. This suspension culture vessel with 125 ml capacity is equipped with features which ensure optimal stirring with low levels of shear stress and enhanced aeration and agitation of spheroid suspension. This system allows easy scale up for larger vessel sizes culture systems. The use of this culture system allows the production of a large number of homogeneous colon cancer spheroids within the same batch [164].

The cultures were followed during 12 days and, cell concentration and spheroid size and number were monitored along time. The results obtained for the optimized culture conditions are presented in Figure 3.8.

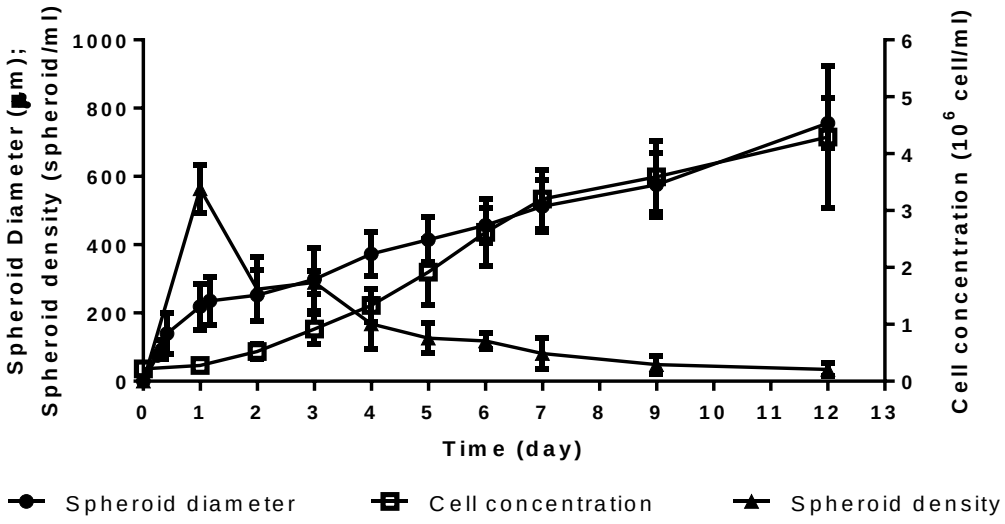

Figure 3.8: HT29 spheroid culture characterization in stirred culture systems. Monitoring of spheroids diameter, concentration and total cell concentration in culture. Data are mean ± SD of four independent experiments.

Average spheroid diameters in suspension culture system were measured based on microscope fluorescence images (Figure 3.10), obtaining a diameter distribution histogram for each daily time point (Figure 3.9). Along the culture, it is possible to verify a gradual increase in cell concentration due to the proliferative character of colon cancer cells.

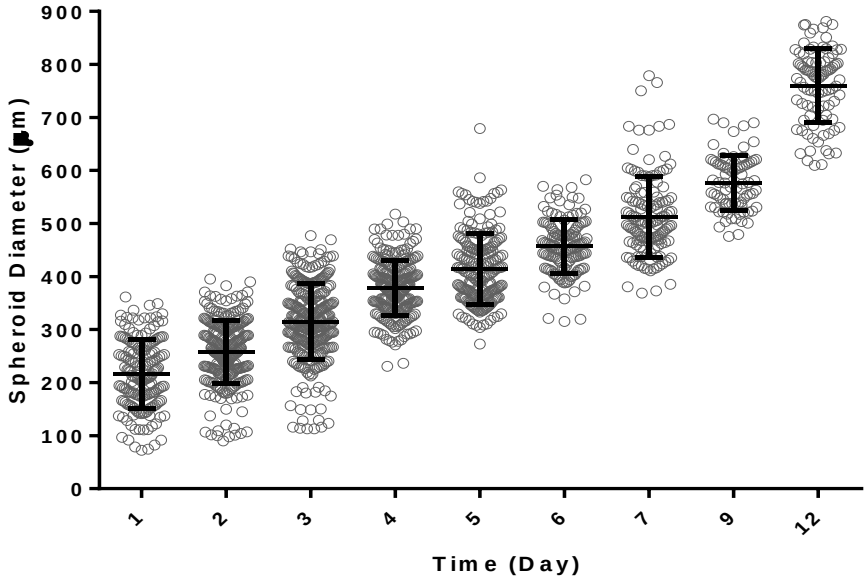

Figure 3.9 : HT29 spheroid size distribution along culture time in stirred culture system. Spheroid feret diameter was determined as described in section 3.4.3. Results were mean ± SD of four independent experiments. All the means present significant difference with $P<0.0001$ by one-way ANOVA analysis.

Spheroid culture viability was assessed using a dual staining with FDA and PI. Non-viable cell were stained in red and viable in green stain (section 2.3.5). The results obtained by fluorescence and bright field microscopy of HT29 spheroids along the culture time are presented in Figure 3.10.

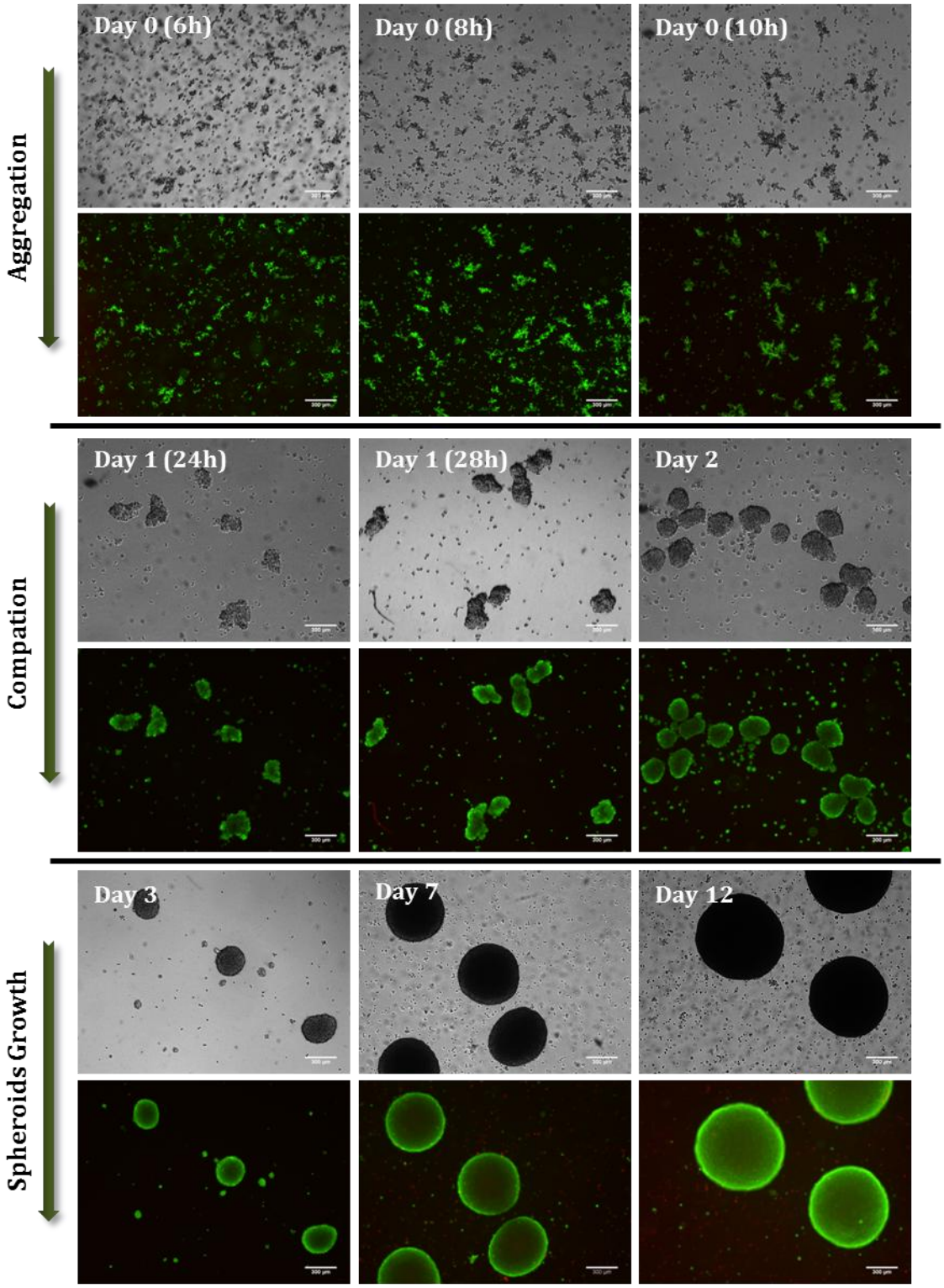

Figure 3.10 : Monitoring of 3D HT29 cultures, along culture time. Phase contrast and fluoresce microscopy images. Viable cells were stained with FDA (green) and non-viable cells were stained with PI (red). Data is from one representative 3D culture of four experiments (scale bar=300 µm)

During culture time it was possible to distinguish three distinct phases: an initial aggregation phase, followed by spheroid compaction and a third phase characterized by spheroid growth.

The early stage of culture corresponded to the aggregation step of HT29 cells. Aggregation took place in the first 24 hours of culture and it was mainly characterized by maintenance of cellular concentration, accompanied by an increase in the spheroid size. The HT29 cell line presented a fast aggregative character and 6 hours of inoculation, spheroids could already be found in suspension (Figure 3.8). At this point, the culture was composed by a heterogeneous population of cells, containing both small cell spheroids as well as floating single cells (Figure 3.10). HT29 cells continued to aggregate until 24 h post-inoculation and the diameter of the spheroids increased rapidly (average diameter of 200 μm, Figures 3.8 and 3.9). During this period cellular concentration was maintained (Figure 3.8), suggesting that the observed increase in spheroid diameter was due to cell aggregation and aggregates fusion.

Between the 1st and 2nd day, a 2-fold increase in cell concentration was observed, although spheroid diameter was kept stable which indicated that spheroid compaction was occurring. Moreover, the decrease in spheroid density observed from day 1st day also suggests the occurrence of spheroid fusion (Figure 3.8).

From the 3rd day onwards, spheroid diameter increased, together with an increase in cell concentration. In addition, during this period (day 3 onwards), spheroids presented low light penetration, evidenced by the darker appearance of spheroids, suggesting a high level of compaction of spheroids (Figure 3.10). It was observed that high viability was maintained along the process, with cells stained with PI being a small minority, mostly in the first culture days during aggregation and compaction (Figure 3.10).

In sum, after the optimization, the aggregation was achieved and multicellular tumor spheroids were obtained with high cellular viability along the culture. The selected method for generation of 3D colon cancer model displays several advantages. Comparing to static culture systems-based methods to obtain spheroids, this system allowed the achievement of compact colon cancer spheroids in a shorter amount of time [128]. Furthermore, the utilization of spinner vessels allowed the generation of a high number of spheroids, for further characterization and utilization in several assays. In addition, this culture system is compatible with live monitoring of the 3D models, with frequent non-destructive sampling and assessment of the properties of the spheroids at different stages of progression.

3.2.2 Phenotypic characterization

The 3D cell model generated in this thesis work was phenotypically characterized along the culture time by flow cytometry and immunofluorescence microscopy.

Firstly, cancer stem cells (CSCs) in both, 2D and 3D, cultures were quantified by assessing the expression of CD44 using flow cytometry. The study was carried out with HT29 cells from tumor spheroids collected at third day of 3D culture, after the aggregation and compaction phase. For the analysis of the cell population by flow cytometry, tumor spheroids were dissociated into a single cell suspension using enzymatic dissociation, as described in section 2.3.5.

The results presented in Figure 3.11 indicate a highly enriched $CD44^+$ cell population for both culture systems. HT29 spheroids at day 3 of 3D culture (Figure 3.11(A)) presented 97.89 ± 0.80 %, and for 2D monolayer culture (Figure 3.11 (B)) 98.81 ± 0.20 % of $CD44^+$ cells.

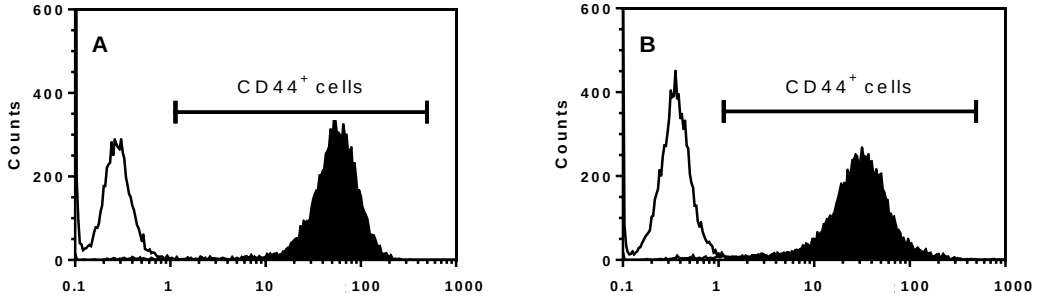

Figure 3.11: Flow cytometry analysis of CD44 expression in HT29 cells cultured in 2D (A) and 3D conditions at day 3 of culture (B). Results from one representative experiment of 3 independent assays.

Quantification of CD44 cell marker suggested a high percentage of CSCs in 2D and 3D cultures. CD44 is consistently overexpressed in colorectal cancer and other types of carcinomas. This membrane receptor recognizes chemoatractants and cytokines responsible for cell motility and invasion [165]. CSCs are identified by the expression of specific cell surface markers which includes CD44, but also CD133 and CD166 on colon cancer [166]. Therefore, to confirm the CSC character of these cells, it would be necessary to perform additional characterization for some of these markers. CSCs are often involved in the growth of colon cancer and can be associated with chemotherapeutic resistance and tumor metastasis (section 1.1.3) [167]. This cell population might be the cause of tumor itself, as described in section 1.1 or they can arise by a dedifferentiation process, verified after EMT, which occurs during metastization (section 1.1.2) [168].

HT29 cells in tumor spheroid were further characterized by assessment of epithelial/mesenchymal character at day 3, 7 and 12 of culture by fluorescence microscopy in spheroid cryosections, with immunodetection of β-catenin, cytokeratin 18, E-cadherin, CD44 and vimentin. F-actin was identified by using the fluorescent molecular probe phalloidin (Figure 3.12 and Figure 3.13).

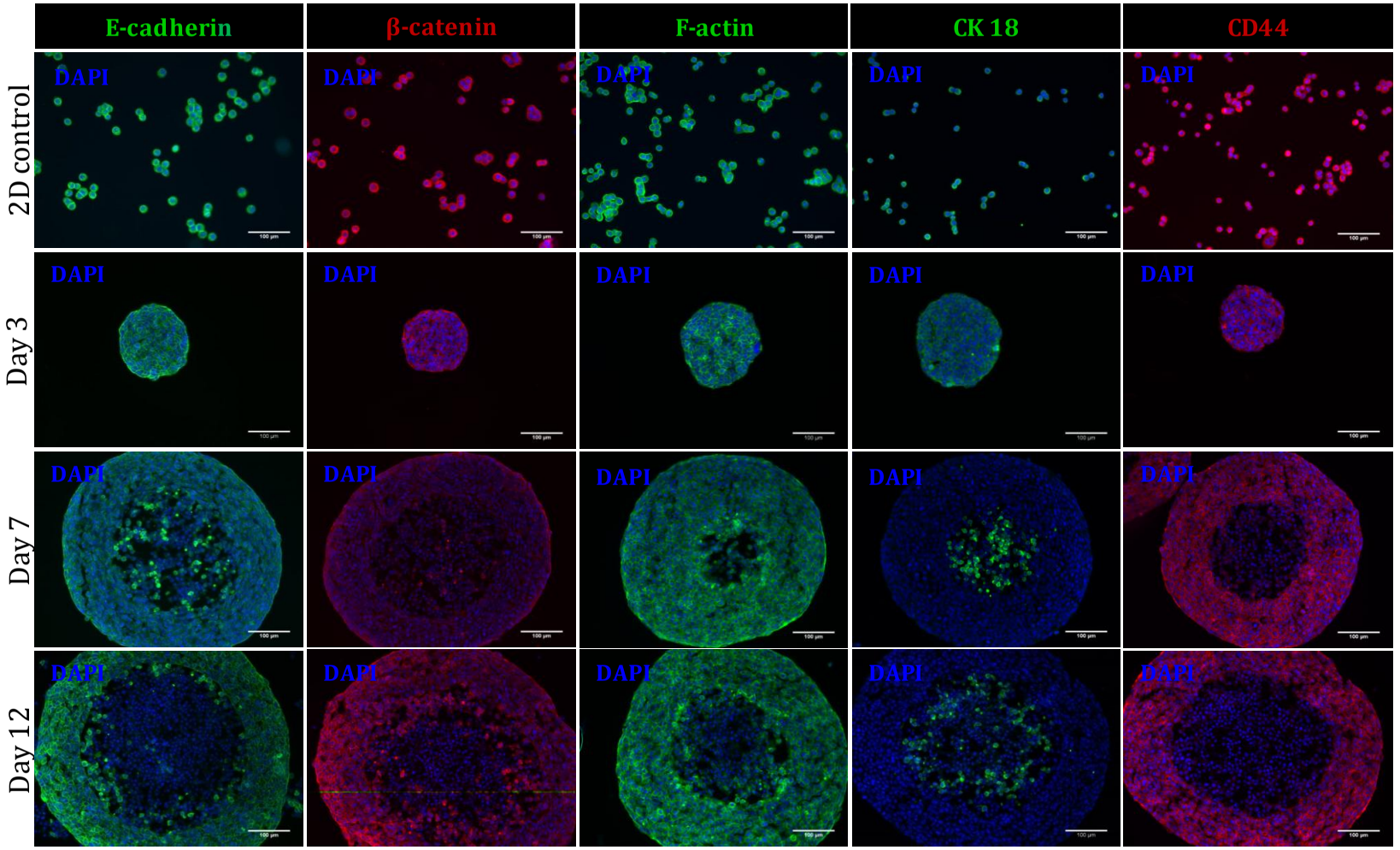

Figure 3.12 : Characterization of HT29 3D cultures by immunofluorescence microscopy. Detection of β-catenin, E-cadherin, F-actin, cytokeratin 18 and CD44 along spheroids growth process (day 3, 7 and 12). DAPI was used to stain nuclei.

The results revealed obvious differences in spheroids along culture time. At an early stage of culture (day 3), spheroids were small and homogeneous. In contrast, larger spheroids (day 7 and 12) exhibited a heterogeneous structure with high compacted cells in spheroid periphery and low compacted cells in spheroid center (Figure 3.12).

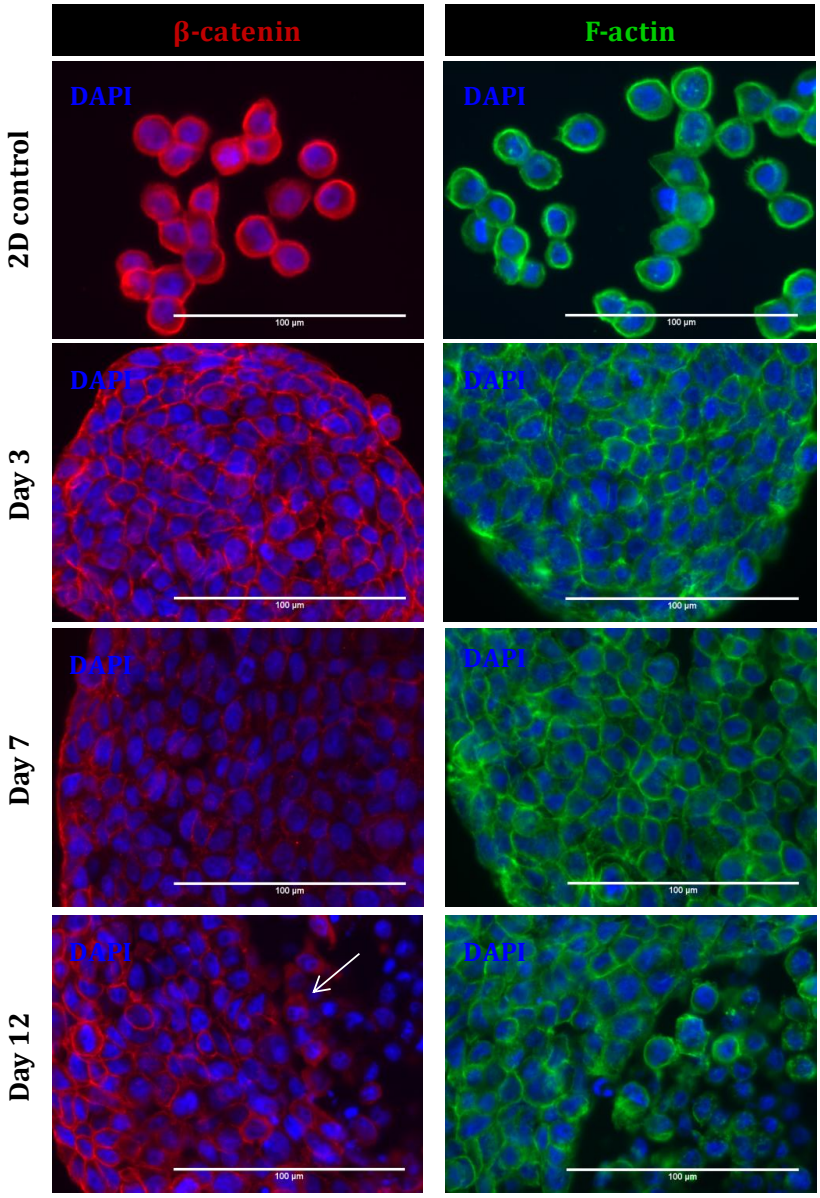

Figure 3.13: Characterization of HT29 spheroids by immunofluorescence microscopy. High magnification images of β-catenin and F-actin detection. Nuclei were labeled with DAPI. White arrow indicates non-membranar β-catenin location.

Results concerning epithelial markers (Figure 3.12 and Figure 3.13) indicated that up to day 7, the spheroid cellular population exhibited epithelial characteristics, positive for E-cadherin and where β-catenin was mostly found in the membrane. Nonetheless, at day 12 of culture, HT29 cells located in the central area of spheroids lost the expression of E-cadherin, while β-catenin was detected in the cytosol (Figure 3.13, white arrow).

F-actin was also detected in tumor spheroids, under the form of an actin ring in the membrane area, except in the center of spheroids with 12 days of culture, in which it

presented a cytoplasmic punctate pattern (Figure 3.13). This pattern may indicate apoptotic activity, as f-actin cleavage has been described associated with this type of cell death [169].

Concerning CK18 expression, differences were observed between day 3 and day 7/12 of culture (Figure 3.12). Indeed, at day 3 there was strong detection distributed through the whole tumor spheroid, in accordance with the epithelial phenotype previously described for of HT29 cells [170]. However, in spheroids collected at day 7 and day 12 of culture CK18 was detected only in the central area of the spheroids. These larger spheroids also presented a positive staining for CD44, exclusively in the peripheral region.

The mesenchymal phenotype of HT29 cell spheroids were evaluated by immunofluorescence microscopy of vimentin and the results are presented in Figure 3.14.

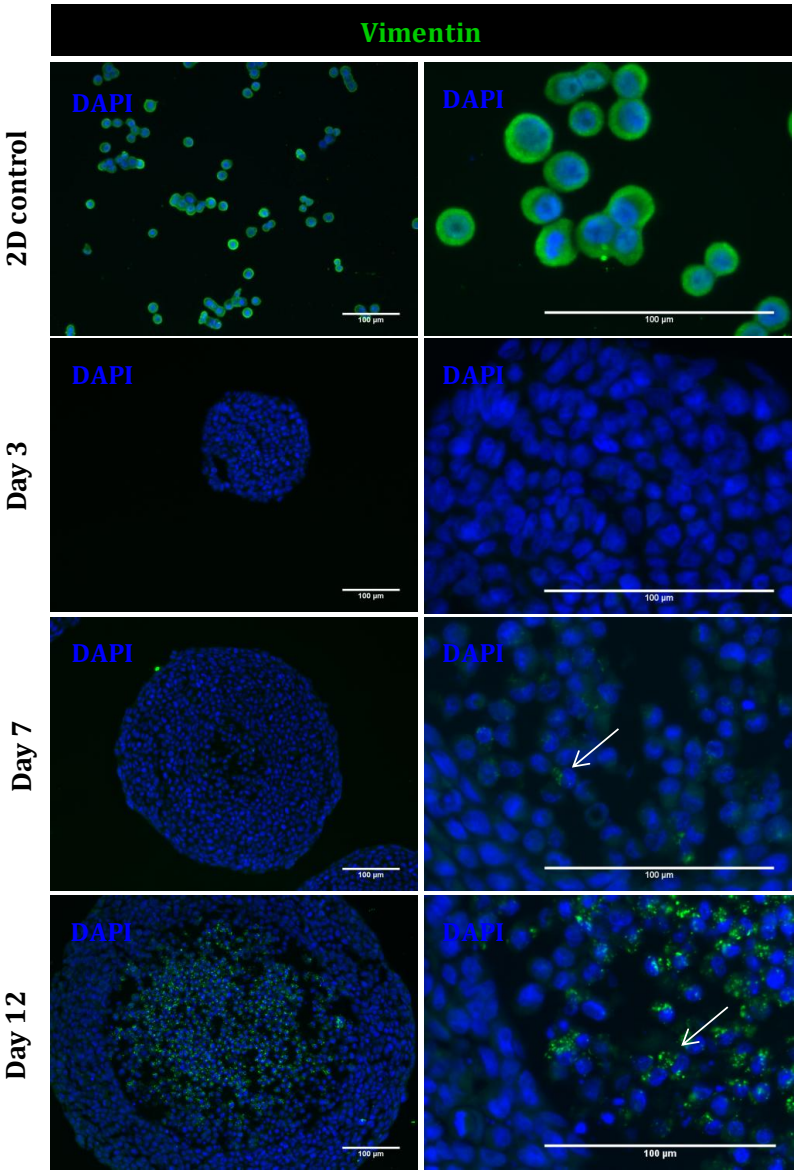

Figure 3.14 : Characterization of 3D cultures by immunofluorescence microscopy. Identification of vimentin along culture time (day 3, 7 and 12). In the right side are presented the respective magnified images. DAPI was used to stain nuclei. White arrows indicate vimentin punctate pattern.

Results showed that HT29 spheroids cells at day 3 of culture did not expressed vimentin, in contrast with spheroids collected at day 7 and 12 which presented a punctate pattern in the central area (Figure 3.14 (white arrows)). This labeling pattern suggested that vimentin was in a cleaved form due to proteolysis. This is a common sign of apoptotic activity, in which vimentin is cleaved by active caspases leading to cell apoptosis [171].

Therefore, to evaluate apoptosis in the tumor spheroids, a form of CK18 cleaved by caspase-3 was detected using a specific antibody (M30 antibody). Figure 3.15 shows the M30 staining of apoptotic cells.

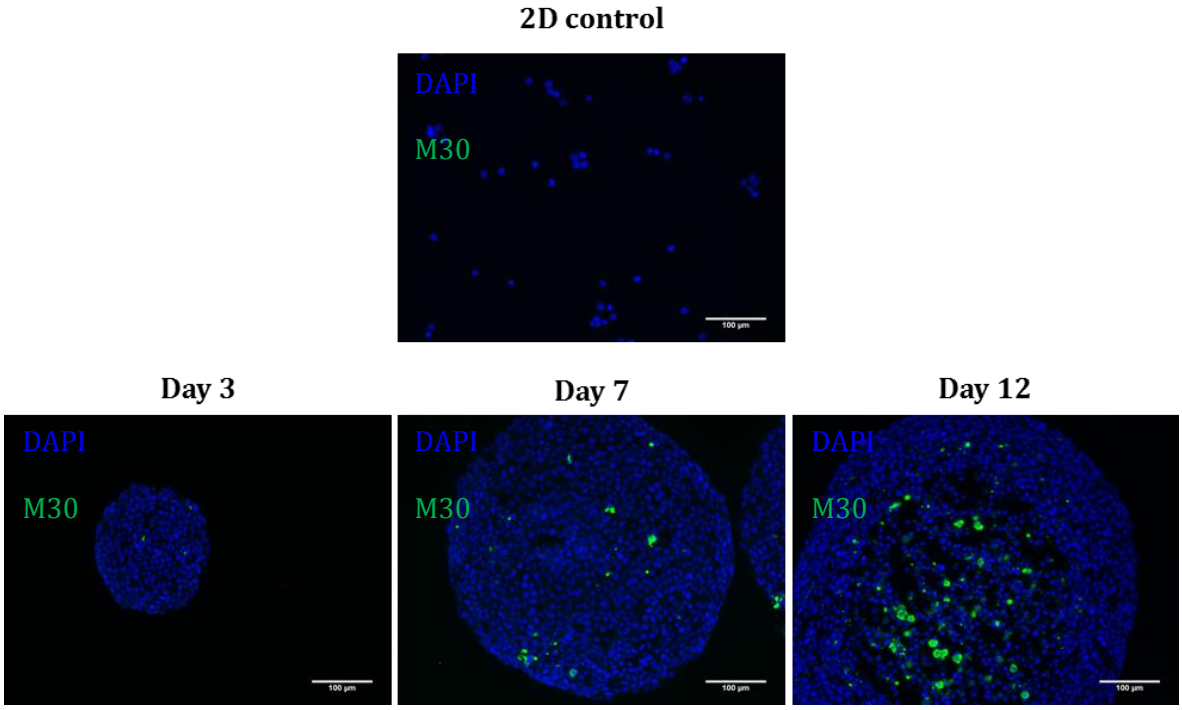

Figure 3.15 : Characterization of 3D cultures by immunofluorescence microscopy. Detection of early apoptotic cells using M30cytodeath marker, along culture time (day 3, 7 and 12). DAPI was used to stain nuclei

The results suggested the existence of relevant apoptotic activity in the core of spheroids at day 12 of culture. As CK18 was not detected in the peripheral layer of spheroids at day 7 and 12 of culture, it was not possible to conclude about apoptotic activity in the spheroids periphery. Nonetheless, at day 12 of culture, spheroids exhibited about 800 µm of diameter, which most probably limited mass transfer of nutrients and oxygen, even in stirred culture systems. Besides, the accumulation of toxic metabolites in the core area might also contribute to the induction of apoptosis [121].

Detection of relevant cell markers expression is summarized on Table 3.5, as well as their respective location in the colon cancer spheroid.

Table 3.5: Cell markers localization along the culture time.

		Cell marker localization on spheroid (core/periphery)			
Culture		**E-cadherin**	**Vimentin**	**CK 18**	**CD44**
	2D	+	+	+	+
3D	Day 3	+/+	-/-	+/+	+/+
	Day 7	+/+	-/-	+/-	-/+
	Day 12	-/+	+/-	+/-	-/+

In general, it was observed relevant phenotypic alterations mainly between spheroids collected at day 3 of culture and spheroids collected at day 7 and 12.

A consistently expression of CD44 and vimentin by HT29 cells, in 2D cultures, can be related with a prior EMT, which is associated to the generation of cancer cells with a stem cell character and phenotype [27]. The expression of CD44 can also be due to the tumor cellular origin, as colon tumors originated in crypt stem cells usually present stem cell markers in the primary tumor [6].

In cell spheroids CD44 detection was limited to the outer layer of the tumor spheroid at later culture stages. This result, combined with the loss of detection of the epithelial marker CK18 suggests the occurrence of a dedifferentiation process, and it could be correlated with *in vivo* tumors which exhibit a dedifferentiated invasive front [172].

E-cadherin expression was frequently detected in spheroid areas of higher cellular compaction, due to their crucial role in maintenance of cell-cell contacts. Spheroids at day 12 of culture revealed a greater area of low compaction in the center of the spheroid, which lack the cell-cell contacts. Herein, E-cadherin expression was not detected which may be explained by the loss of cell-cell contacts [173].

E-cadherin and cytokeratin 18 (CK18) are generally found in adenocarcinomas which present an epithelial phenotype [170, 173]. Thus, tumor cells with epithelial characteristics show a positive staining for E-cadherin, a trans-membrane adhesion receptor required to form and maintain adherens junctions (AJs) and for CK18 which is a cytoskeleton protein with an important role in maintaining cell shape and internal organization [170]. The loss of E-cadherin and other epithelial characteristic proteins, such as cytokeratins, can be associated with the transition to a mesenchymal character or with the loss of cell-cell contacts in the core of the spheroid. Usually, when cancer cells acquires an invasive phenotype, they lose the adhesion with surrounding cells and decrease cytoskeleton proteins expression [170].

Alterations in F-actin (filamentous actin, another structural protein,) which displays a crucial role in the maintenance of epithelial cells polarity through the actin bundles, can also be related with EMT process. These bundles are lost when colonic cancer cells become unpolarized and acquire motility [174, 175]. In this case, it is possible to identify actin filaments in cell cytoskeleton which can be involved in cell movement [176]. However, immunofluorescence microscopy of cells stained with f-actin only revealed some evidences of apoptotic activity at day 12, due probably to hypoxic conditions.

As well as F-actin, β-catenin cellular location can also change when EMT occurs. β-catenin can be identified in cellular membrane by immunofluorescence microscopy if cancer cells which present an epithelial phenotype and express E-cadherin (section 1.1.2). When the cell loses the E-cadherin expression, β-catenin is translocated into de nucleus or it may be also found diffusely distributed in the cytoplasm [25].

Besides the loss of epithelial characteristics, it is usual to find mesenchymal characteristic proteins, such as vimentin, in cells that undergo EMT. Vimentin is a type III intermediate filament which plays an important role in supporting the position of the organelles in cytosol and offers cell flexibility. Often, vimentin is expressed in epithelial invasive late carcinomas [177]. The expression of vimentin was identified in HT29 cells cultured in 2D and it was lost when cells were cultured in 3D spheroids. However, at day 12 of culture, it was detected a punctate pattern of vimentin in the core of spheroids, in association with the loss of membrane β-catenin. These results suggest that these cells probably undergone EMT. The evidence of EMT in spheroids core cells might be linked with the hypothesis that this area presents hypoxic conditions. Higgins et al. have demonstrated that EMT may be induced by hypoxia in renal epithelial cells [178]. In addition, to provide conclusions about the occurrence of EMT, further studies have to be performed using additional cell markers.

The characterization of the obtained 3D model along culture time allowed to establish a relation with some of the features observed in tumor progression *in vivo*. Spheroids collected at day 7 or 12 presented a higher similarly degree with malignant tumors, with less differentiated cells located in the cancer's outer area, while presenting an apoptotic/necrotic center due to diffusion limitations. These older spheroid microregions could simulate micrometastases or intervascular microregions of larger tumors [144]. Hence, it is possible to mimic multiple cancer stages according to the type of study.

Indeed, 3D model characterization allows concluding about the type of cancer model used in the *in vitro* anticancer assays, as well as establishing a relation between the characteristics of this *in vitro* model and *in vivo* tumor stage.

3.3 Evaluation of anticancer potential of natural extracts using 3D cell models

In the final part of this work the most promising natural extracts selected from 2D antiproliferative assays (section 3.1) were evaluated for their anticancer potential using the 3D cell model developed previously (section 3.2). The biological activity of orange peel and Brooks cherry extracts was assessed by analyzing i) antiproliferative effect; ii) cell cycle arrest and iii) induction of apoptosis.

3.3.1 Antiproliferative activity

Antiproliferative effect of Brooks cherry and orange peel extracts was evaluated using HT29 spheroids with different diameters, approximately 300, 400 and 500 µm. The dose-response curves obtained for all samples after 24 hours of incubation are presented in Figure 3.16.

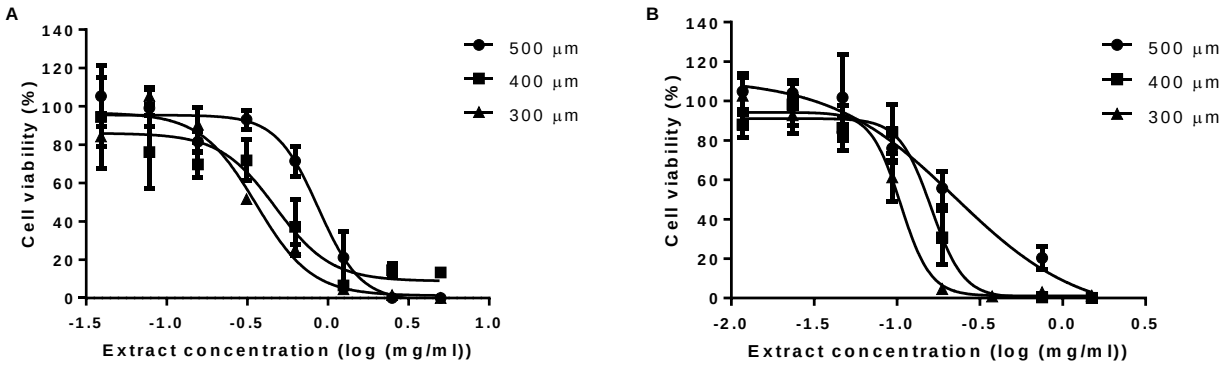

Figure 3.16: Dose-response curves of orange peel (A) and Brooks cherry (B) on HT29 cell spheroids with different sizes (incubation time=24; results are mean ± SD (n=6)).

In addition, perillyl alcohol, the main bioactive compound identified in cherry extracts, was also tested aiming at evaluating the antiproliferative effect of a single compound in this 3D cell model (Figure 3.17).

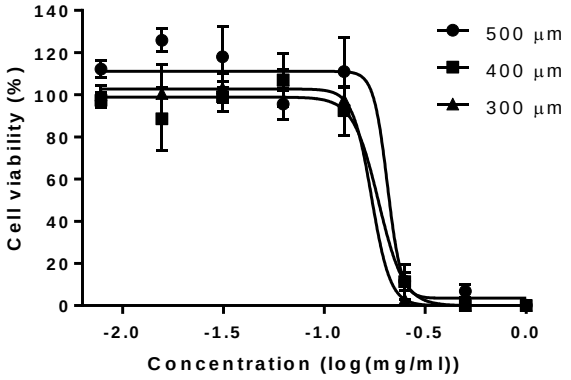

Figure 3.17: Dose-response curves of perillyl alcohol on HT29 cell spheroids with different sizes (incubation time=24; results are mean ± SD (n=6)).

Results showed that the antiproliferative effect of natural extracts was dependent of HT29 spheroid size. This result could be related with the poor diffusion of the main phytochemicals presented in both extract samples, through HT29 spheroid. This effect was not observed for perillyl alcohol, probably due to the low molecular size and the high lipophilic character (see appendix C) that can provides a high diffusion capacity and efficient mass-transfer into cancer cells spheroids [179].

In Table 3.6 are compared the EC50 values of natural extracts and perillyl alcohol obtained using 2D and 3D models of colon cancer cells.

Table 3.6: EC50 values of natural extracts and perillyl alcohol determined using 2D and 3D cell models (incubation time= 24 h).

		EC50 (mg extract/ml)		
		Orange	**Cherry Brooks**	**POH (mg/ml) EC50**
2D model		0.488 ± 0.031	0.092 ± 0.014	0.146 ± 0.037
3D model	300 µm	0.538 ± 0.049	0.105 ± 0.007	0.152 ± 0.056
	400 µm	0.709 ± 0.291	0.161 ± 0.022	0.157 ± 0.021
	500 µm	1.308 ± 0.153	0.224 ± 0.133	0.172 ± 0.030

Overall, results showed that when tested in 3D model both natural extracts decreased their antiproliferative effect (increase of EC50 values). However, the effect was less evident for smaller spheroids (300 µm). As described previously, phenotypical characterization of smaller spheroids showed multiple resemblances with monolayer culture cells (section 3.2.2). In addition, the spheroids with 300 µm of diameter are less compacted than 400 and 500 µm cell spheroids and thus, the diffusion of the main bioactive molecules were probably not affected in 300 µm spheroids. Regarding tumor spheroids with 500 µm of diameter, the EC50 values of both extracts increased more than two times in relation to 300 µm spheroids. Furthermore, 500 µm spheroids displayed characteristics observed in *in vivo*

carcinoma, such as the hypoxic/apoptotic core and less differentiated cells in the surrounding area, which confers chemotherapeutic resistance [140]. These characteristics, combined with mass transport limitations as observed in this size of spheroid, can be the cause of greater resistance to the extracts treatment [140].

By contrast, the EC50 values for perillyl alcohol obtained in 2D and 3D cell based assays were similar, reinforcing the high permeability and diffusion properties of this compound through HT29 cell spheroids.

Aiming at evaluating if the incubation time improved the antiproliferative response of natural extracts, HT29 cell spheroids were incubated with the tested extracts for 72 hours.

In Figure 3.18 is presented the EC50 values determined for incubations with natural extracts for 72 hours. Results were compared with EC50 data obtained for 24 hours of incubation.

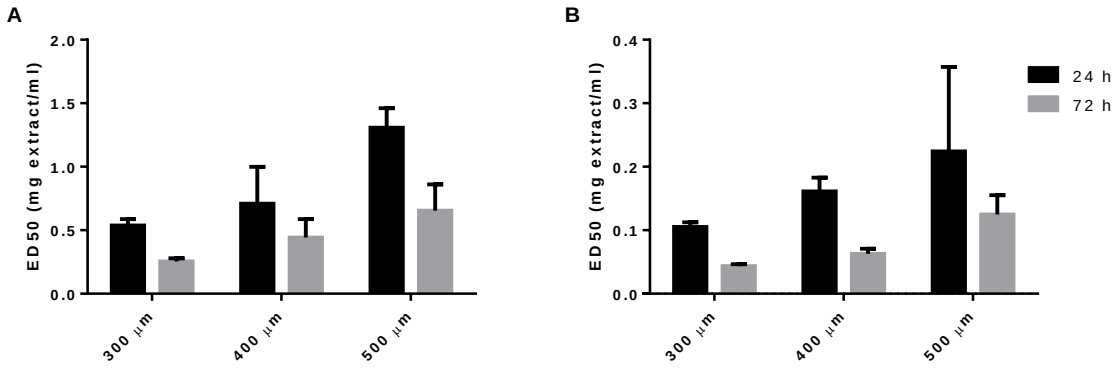

Figure 3.18: EC50 values of antiproliferative effect on HT29 tumor spheroids, after 24 and 72 hours of incubation with orange peel (A) and cherry Brooks (B) extract. Data are mean ± SD of nonlinear curve fitting (n=6).

In general, the antiproliferative effect of both extracts was improved after 72 hours of incubation. A decrease of about 2 times on EC50 values recorded at 72 hours was observed in relation to effective doses achieved at 24 hours, for all cell spheroids. These findings suggest that the increase of time exposure leads to a decrease of the therapeutic resistance of tumor spheroids. The diffusion of the main bioactive compounds was probably enhanced by this longer treatment.

The decrease of chemotherapeutic sensibility between 2D and 3D tumor cultures was already verified in prior studies. In particular, for colon cancer tumor spheroids, the chemoresistance was studied for the treatment with several drugs including, 5-FU, oxaliplatin, irinotecan and melphalan. The differences in drug resistance between older spheroids and 2D/early spheroids have been highly associated with the presence of hypoxic regions and with an increased expression of stem cell marker CD44 [140, 163]. Hence, further studies have to be performed in order to assess the influence of CD44 expression in the resistance to extracts therapy.

3.3.2 Cell cycle analysis

Chemotherapeutic drugs may exert their effects by stopping cell replication. This replicative process, cell cycle, comprises four stages: G1 (cell growth phase), S (DNA synthesis), G2 (pre-mitotic phase) and M (cell division by mitosis).

In order to determine whether natural extracts induced a cell cycle arrest of HT29 tumor spheroids, a flow cytometric analysis of cell cycle was performed. Colon cancer spheroids with 500 µm of diameter were selected for this study because at this stage they presented a central necrotic/apoptotic core and a compact outer ring, phenotypic characteristics of a primary tumor in with intravascular microregions *in vivo* (section 3.2.2).

HT29 spheroids were incubated for 24 hours with natural extracts and perillyl alcohol. For all samples, the concentration tested was the one that provided a decrease of 30% in cell proliferation (section 3.3.1). The results are presented in Figure 3.19.

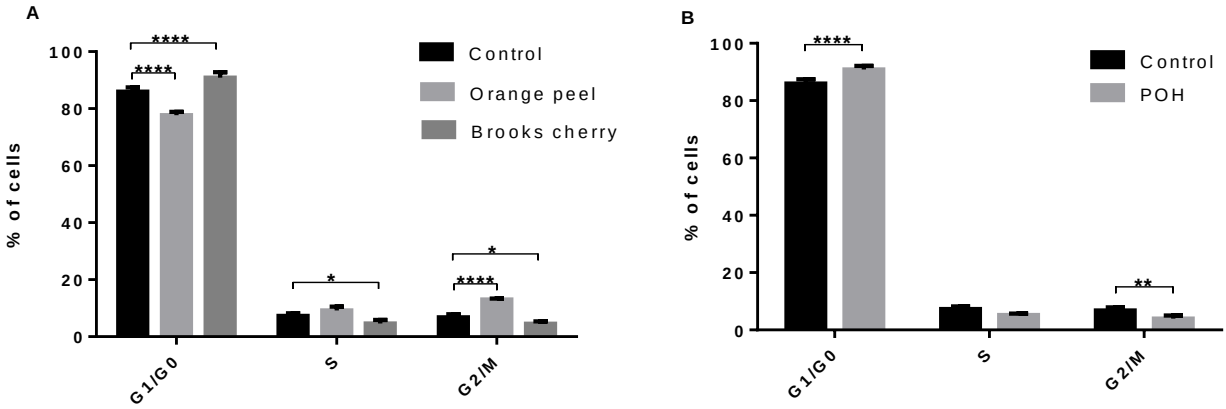

Figure 3.19 : Cell cycle distribution on HT29 cells in the tumor spheroid (diameter=500 µm) after incubation with natural extracts (A) and perillyl alcohol (B) (incubation time=24 h). Results are mean ± SD of four independent experiments. The significant differences are expressed in asterisks (* P<0.5 and**** P<0.0001) by two-way ANOVA analysis.

The results showed that natural extracts induced cell cycle arrest in different cell cycle checkpoints (Figure 3.19(A)). Particularly, cherry Brooks extract induced cell cycle arrest in G1 phase. This effect is in accordance with previous observations using HT29 monolayer culture (2D) and with other cherry extracts presenting similar phytochemical composition [90]. It could be related with the presence of perillyl alcohol demonstrated in previous studies [53], that displayed similar response in HT29 cell spheroids (Figure 3.19 (B)). Also, it is in accordance with previous reports that demonstrated that perillyl alcohol affects the expression of key regulatory proteins of cell cycle (cyclin D1, cyclin E, cdk2 and cdk4) which are involved in G1-S phase transition [98].

For orange peel extract, an induction of cell cycle arrest in the G2/M phase was observed. As described in section 3.1.2, PMFs are the main bioactive compounds present in orange peel extract. These compounds were already reported to induce cell cycle arrest in different cell cycle checkpoints of colon cancer cell lines [73, 83]. In particular, an induction of the G2/M phase was verified by sinensetin in gastric adenocarcinoma cells [83]. Thus, these

compounds could be one of the main contributors for the bioactive effect of orange extract. The other compounds, namely tangeretin and nobiletin, are also reported to induce cell cycle arrest in HT29 but in different cell cycle checkpoints, S and G1 respectively, in human colon adenocarcinoma [73]. These findings suggest that tangeretin and nobiletin may have a low influence on cell cycle regulation of orange extract in HT29 spheroids. This result could be justified with the chemical structure of this compounds that may compromised their diffusion and mass transfer through spheroid. Further studies should be performed in this 3D cell model with these phytochemical compounds, alone and in combination, in order to identify the main bioactive molecules of orange natural extracts.

3.3.3 Apoptosis induction

The effect of phytochemical extracts on induction of apoptosis in HT29 tumor spheroids was assessed through the evaluation of caspase-3 activity, which are proteases that play an essential role in the apoptotic process [180]. For both extracts, assays were performed with different spheroid sizes using the EC50 value previously obtained for 300 µm spheroids. In Figure 3.20 are presented the results obtained by fluorescence microscopy of the cell spheroids.

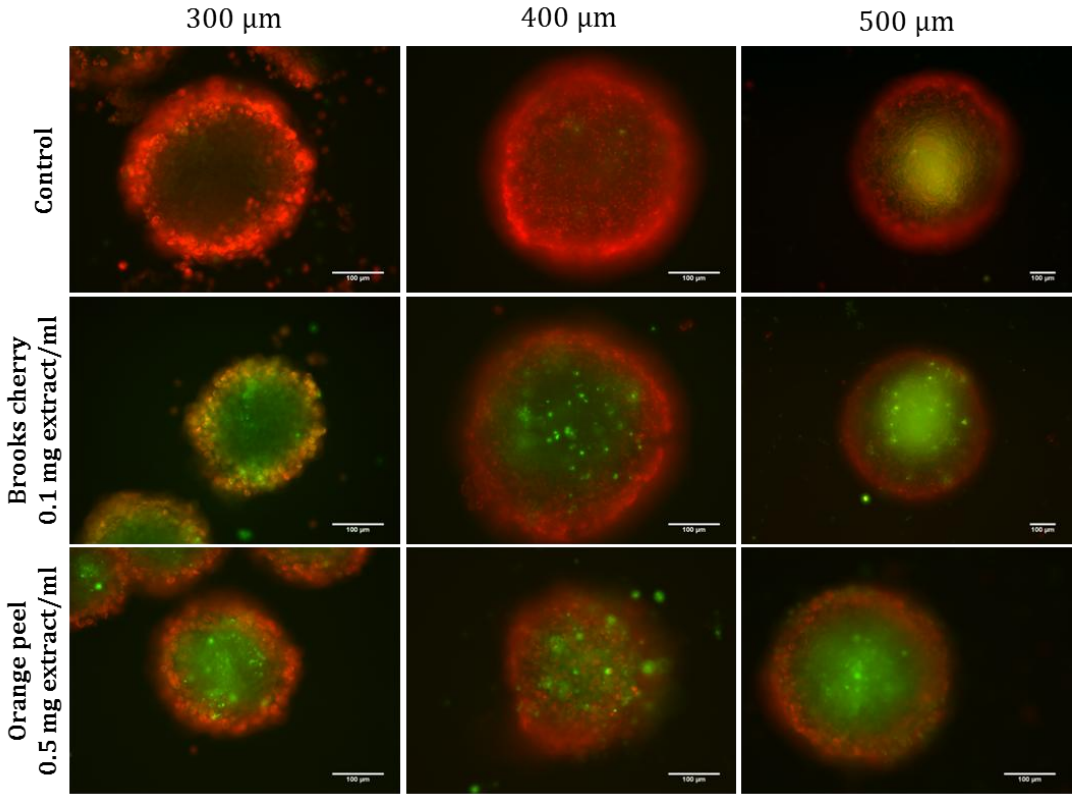

Figure 3.20: Evaluation of apoptotic activity on HT29 cells in tumor spheroids incubated with natural extracts by fluorescence microscopy (incubation time=24 h). Detection of capase-3 (green) and mitochondrial activity (red) for spheroids with 300, 400 and 500 µm of diameter.

The results showed that natural extracts induced apoptosis in HT29 spheroids. It is important to note that this effect was more pronounced in smaller spheroids (300 μm), which is in accordance with the antiproliferative results. However, for spheroids with 400 and 500 μm of diameter, it was suggested that the apoptotic effect was more pronounced in the surface cells, in contrast to core cells which seem to be less affected. As discussed previously, the lowest anticancer effect observed for higher HT29 spheroid sizes could be related with mass transfer limitations of the main bioactive compounds of the extracts.

In fact, images obtained with confocal microscope of HT29 spheroids incubated with orange peel extract revealed that apoptotic effect was more pronounced in cells located at the spheroid surface (Figure 3.21).

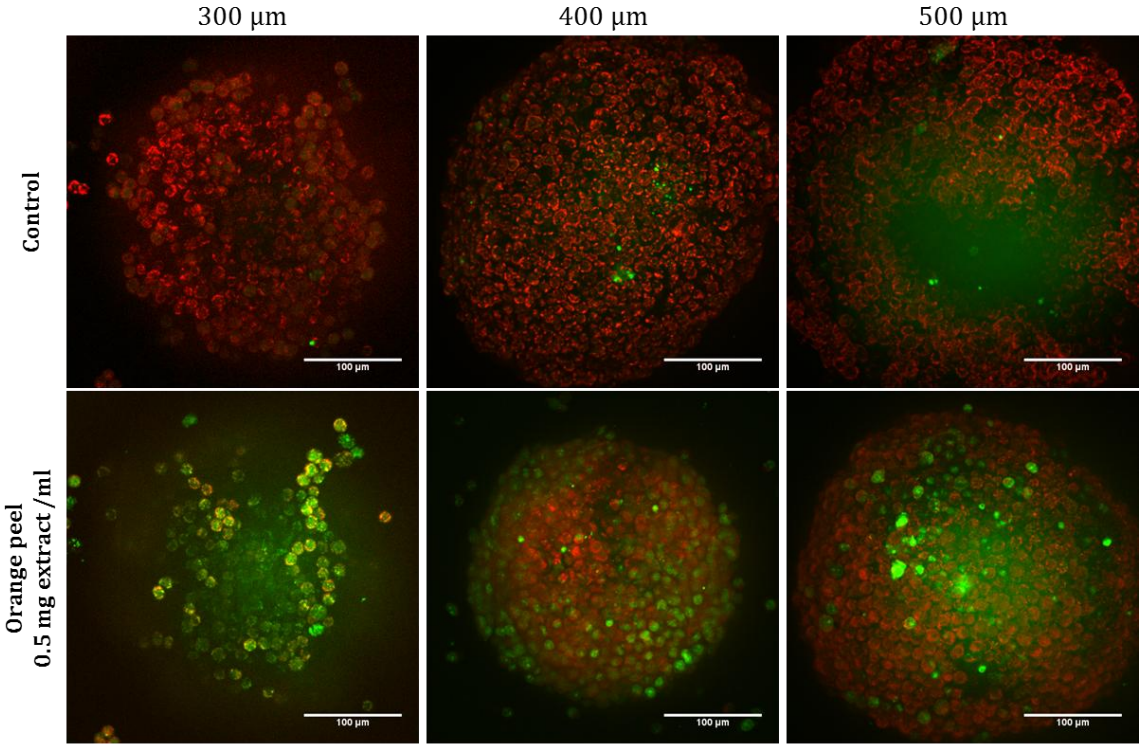

Figure 3.21: Evaluation of apoptotic activity on HT29 cells in tumor spheroids incubated with orange peel extract by fluorescence confocal microscopy (incubation time=24 h). Detection of capase-3 (green) and mitochondrial activity (red) for spheroids with 300, 400 and 500 μm of diameter.

After 24 hours of orange peel extract treatment, spheroids presented a clear increase in apoptotic activity. In particular, for spheroids with 300 μm of diameter, it were detected a large number of apoptotic cells, suggesting that the majority of spheroids cells undergo apoptosis. These results reinforce the evidences of sinensetin contribution for the anticancer effect of orange peel extract. For this PMF the apoptotic effect was reported in human gastric adenocarcinoma and was associated with the up-regulation of proteins involved in the induction apoptosis of tumor cells [83]. The other main compounds, namely tangeretin and nobelitin, were reported to exert a cytostatic effect in colon cancer cell line HT29 with no apoptotic effect [73]. The induction of cell cycle arrest by orange peel extract has already been associated with sinensetin (section 3.3.2) activity and both results are complementary.

It is already reported the apoptotic effect of perillyl alcohol, which could be correlated with the high apoptotic effect observed after 24 hours of treatment with Brooks cherry extract. In lung adenocarcinoma, perillyl alcohol shows to increase the activity of caspase-3, as well as to increase the expression of other regulatory proteins related with the apoptotic process [181].

Furthermore, it is important to note that control spheroids, collected at day 7 of culture, revealed a diffuse green fluorescent staining which appear to be located in the core of the spheroid. These results emphasize the evidence that cells undergo apoptosis in the core of the spheroid due to their larger diameter of the spheroids (section 3.2.2). However, the detection of this apoptotic region using this capase-3 cellular marker has to be further investigated in order to provide specific conclusions. Additional apoptosis assays, using spheroids cryosections, would be carried out with and without extracts exposure.

4 Conclusion

In the present study, natural extracts obtained by clean extraction methodologies from fruit residues were investigated for their anticancer potential aiming at identifying promising bioactive molecules for the development of natural chemotherapeutic agents towards colon cancer.

Among 14 natural extracts screened in a 2D model of HT29 colorectal cancer cells, orange peel and Brooks cherry extracts distinguished for presenting higher antiproliferative effect. These extracts were produced by high pressure technology that revealed to be an efficient process to extract and isolate potent bioactive molecules namely perillyl alcohol and polymethoxylated flavones from sweet cherries and orange peels, respectively. The potential anticancer effect of these natural extracts were also validated in a 3D model of HT29 cell spheroids, which showed similarities with *in vivo* tumor, including similar phenotypes and resistance to chemotherapy agents. Orange peel and cherry extracts inhibited colon cancer cells proliferation and promoted apoptosis in HT29 spheroids, and this effect was dependent with the tumor spheroid size. Moreover, natural extracts induced cell cycle arrest in different cell cycle checkpoints - cherry extract induced cell cycle arrest at G1 phase while orange peel extract induced at G2/M phase- which was correlated with their phytochemical composition.

Overall, the use of colorectal cancer cell spheroids constitutes an improved and feasible alternative to the classic 2D cellular model to evaluate and understand the chemotherapeutic potential of bioactive molecules and phytochemical-rich extracts towards colon cancer. Future studies should be performed in order to establish relationship between natural extracts activity and cellular phenotypical alterations in this 3D cancer cell model. Moreover, a better identification of the main bioactive compounds as well as their structure is required to further understand the chemotherapeutic effect and mechanisms of natural compounds.

5 References

1. Ferlay, J., et al., *GLOBOCAN 2008 v2.0, Cancer Incidence and Mortality Worldwide: IARC CancerBase No. 10 [Internet].* Lyon, France: International Agency for Research on Cancer; 2010. Available from: http://globocan.iarc.fr, accessed on 13/04/2013.
2. Siegel, R., D. Naishadham, and A. Jemal, *Cancer statistics, 2013.* CA: A Cancer Journal for Clinicians, 2013. **63**(1): p. 11-30.
3. *European Age-Standardised rates calculated by the Cancer Research UK Statistical Information Team, 2011, using data from GLOBOCAN 2008 v1.2, IARC. http://globocan.iarc.fr.*
4. *American Cancer Society. Colorectal Cancer Facts & Figures 2011-2013. Atlanta: American Cancer Society, 2011.*
5. Crosnier, C., D. Stamataki, and J. Lewis, *Organizing cell renewal in the intestine: stem cells, signals and combinatorial control.* Nat Rev Genet, 2006. **7**(5): p. 349-59.
6. Humphries, A. and N.A. Wright, *Colonic crypt organization and tumorigenesis.* Nature Reviews Cancer, 2008. **8**(6): p. 415-424.
7. Heber, D., et al., eds. *NUTRITIONAL ONCOLOGY*. 2006, Academic Press-Elsevier.
8. Ruddon, R., *Cancer biology*. 4 ed. 2007: Oxford.
9. Castells, A., H. Harada, and A.K. Rustgi, *Colorectal Cancer*, in *Encyclopedia of Genetics*, A. Press, Editor. 2001. p. 422–423.
10. Fausto, V.K.A.K.A.N., *ROBBINS AND COTRAN PATHOLOGIC BASIS OF DISEASE, 7TH EDITION*. 2005: Saunders.
11. http://www.medinfo.net/imi/tissue-areas/colorectal/, accessed on 10/06/2013
12. Fearon, E. and B. Vogelstein, *A genetic model for colorectal tumorigenesis.* Cell, 1990. **61**(5): p. 759-767.
13. OIKONOMOU, E. and A. PINTZAS, *Cancer Genetics of Sporadic Colorectal Cancer: BRAF and PI3KCA Mutations, their Impact on Signaling and Novel Targeted Therapies.* ANTICANCER RESEARCH, 2006. **26**: p. 1077-1084.
14. Mutch, M.G., *Molecular profiling and risk stratification of adenocarcinoma of the colon.* Journal of Surgical Oncology, 2007. **96**(8): p. 693-703.
15. Yeatman, T.J., *Colon Cancer.* ENCYCLOPEDIA OF LIFE SCIENCES, 2001: p. 1-6.
16. Potter, J.D., *Colorectal cancer: Molecules and populations.* Journal of the National Cancer Institute, 1999: p. 91:916.
17. Farin Amersi, M.D., et al., *Colorectal Cancer: Epidemiology, Risk Factors, and Health Services.* CLINICS IN COLON AND RECTAL SURGERY, 2005. **18**(3): p. 133-140.
18. Burt, R., J. DiSario, and L. Cannon-Albright, *Genetics of colon cancer: impact of inheritance on colon cancer risk.* Annu Rev Med, 1995. **46**: p. 371-379.
19. Yamaguchi, H., J. Wyckoff, and J. Condeelis, *Cell migration in tumors.* Current Opinion in Cell Biology, 2005. **17**(5): p. 559-564.
20. Thiery, J.P., *Epithelial–mesenchymal transitions in tumour progression.* Nature Reviews Cancer, 2002. **2**: p. 442-454.
21. Chambers, A.F., A.C. Groom, and I.C. MacDonald, *Metastasis: Dissemination and growth of cancer cells in metastatic sites.* Nature Reviews Cancer, 2002. **2**(8): p. 563-572.
22. Friedl, P. and K. Wolf, *Tumour-cell invasion and migration: diversity and escape mechanisms.* Nature Reviews Cancer, 2003. **3**(5): p. 362-374.
23. Steeg, P.S., *Metastasis suppressors alter the signal transduction of cancer cells.* Nature Reviews Cancer, 2003. **3**: p. 55-63.
24. Bates, R.C. and A.M. Mercurio, *The Epithelial-Mesenchymal Transition (EMT) and Colorectal Cancer Progression.* Cancer Biology & Therapy, 2005. **4**(4): p. 365-370.

25. Gavert, N. and A. Ben-Ze'ev, *Epithelial–mesenchymal transition and the invasive potential of tumors.* Trends in Molecular Medicine, 2008. **14**(5): p. 199-209.
26. Weinberg, R.A., *The Biology of Cancer*. 2007: New York.
27. Mani, S.A., et al., *The Epithelial-Mesenchymal Transition Generates Cells with Properties of Stem Cells.* Cell, 2008. **133**(4): p. 704-715.
28. Makin, G. and C. Dive, *Apoptosis and cancer chemotherapy.* TRENDS in Cell Biology, 2001. **11**(11): p. s22-s26.
29. Sarkar, F.H., *Using Chemopreventive Agents to Enhance the Efficacy of Cancer Therapy.* Cancer Research, 2006. **66**(7): p. 3347-3350.
30. Hanahan, D. and Robert A. Weinberg, *Hallmarks of Cancer: The Next Generation.* Cell, 2011. **144**(5): p. 646-674.
31. Caley, A. and R. Jones, *The principles of cancer treatment by chemotherapy.* Surgery (Oxford), 2012. **30**(4): p. 186-190.
32. Connors, T.A., R. Duncan, and R.J. Knox, *The Chemotherapy of Colon Cancer.* European Journal of Cancer, 1995. **31A**: p. 1373-1378.
33. Price, P., K. Sikora, and T. Illidge, *Treatment of Cancer*. 2008: London.
34. Dean, M., T. Fojo, and S. Bates, *Tumour stem cells and drug resistance.* Nature Reviews Cancer, 2005. **5**(4): p. 275-284.
35. G R Hamilton, T.F.B., *In the arms of morpheus: the development of morphine for postoperative pain relief.* Canadian Journal of Anesthesia, 2000. **47**(4): p. 367-374.
36. Harvey, A., *Natural products in drug discovery.* Drug Discovery Today, 2008. **13**(19-20): p. 894-901.
37. Li, J.W.H. and J.C. Vederas, *Drug Discovery and Natural Products: End of an Era or an Endless Frontier?* Science, 2009. **325**(5937): p. 161-165.
38. Cragg, G.M. and D.J. Newman, *Biodiversity: A continuing source of novel drug leads.* Pure and Applied Chemistry, 2005. **77**(1): p. 7-24.
39. *World Health Organization media center. Traditional medicine. Fact sheet nº134, 2008* [http://www.who.int/mediacentre/factsheets/fs134/en/] (Accessed on 1/09/ 2013).
40. Ngo, L.T., J.I. Okogun, and W.R. Folk, *21st Century natural product research and drug development and traditional medicines.* Natural Product Reports, 2013. **30**(4): p. 584.
41. Butler, M.S., *Natural products to drugs: natural product-derived compounds in clinical trials.* Natural Product Reports, 2008. **25**(3): p. Natural Product Reports.
42. Dragnev, K.H., et al., *Uncovering Novel Targets for Cancer Chemoprevention.* Recent Results in Cancer Research, 2007. **174**: p. 235-243.
43. Rajamanickam, S. and R. Agarwal, *Natural products and colon cancer: current status and future prospects.* Drug Development Research, 2008. **69**(7): p. 460-471.
44. Taché, S., A. Ladam, and D.E. Corpet, *Chemoprevention of aberrant crypt foci in the colon of rats by dietary onion.* European Journal of Cancer, 2007. **43**(2): p. 454-458.
45. Miyamoto, S., et al., *Dietary flavonoids suppress azoxymethane-induced colonic preneoplastic lesions in male C57BL/KsJ-db/db mice.* Chemico-Biological Interactions, 2010. **183**(2): p. 276-283.
46. Newman, D.J., *Natural products as leads to potential drugs: an old process or the new hope for drug discovery?* Journal of Medicinal Chemistry, 2008. **51**: p. 2589–2599.
47. Wahle, K.W.J., et al., *Plant Phenolics in the Prevention and Treatment of Cancer.* Advances in experimental medicine and biology, 2010. **698**: p. 36-51.
48. Wang, G., W. Tang, and R. Bidigare, *Terpenoids As Therapeutic Drugs and Pharmaceutical Agents*, in *Natural Products*, L. Zhang and A. Demain, Editors. 2005, Humana Press. p. 197-227.
49. Crowell, P.L., *Prevention and Therapy of Cancer by Dietary Monoterpenes.* The Journal of Nutrition, 1999. **129**(3): p. 775.
50. Lu, J.-J., et al., *Alkaloids Isolated from Natural Herbs as the Anticancer Agents.* Evidence-Based Complementary and Alternative Medicine, 2012. **2012**: p. 12.

51. Cragg, G.M. and D.J. Newman, *Natural products: A continuing source of novel drug leads.* Biochimica et Biophysica Acta (BBA) - General Subjects, 2013. **1830**(6): p. 3670-3695.
52. LI, S., C.-Y. LO, and C.-T. HO, *Hydroxylated Polymethoxyflavones and Methylated Flavonoids in Sweet Orange (Citrus sinensis) Peel.* J. Agric. Food Chem., 2006. **54**: p. 4176-4185.
53. Serra, A.T., et al., *Processing cherries (Prunus avium) using supercritical fluid technology. Part 1: Recovery of extract fractions rich in bioactive compounds.* The Journal of Supercritical Fluids, 2010. **55**(1): p. 184-191.
54. LEA, M.A., et al., *Inhibition of Growth and Induction of Differentiation of Colon Cancer Cells by Peach and Plum Phenolic Compounds.* Anticacer Research, 2008. **28**: p. 2067-2076.
55. Sreekanth, D., et al., *Betanin a betacyanin pigment purified from fruits of Opuntia ficus-indica induces apoptosis in human chronic myeloid leukemia Cell line-K562.* Phytomedicine, 2007. **14**(11): p. 739-746.
56. Guinda, Á., M.C. Pérez-Camino, and A. Lanzón, *Supplementation of oils with oleanolic acid from the olive leaf (olea europaea).* European Journal of Lipid Science and Technology, 2004. **106**(1): p. 22-26.
57. Boudhrioua, N., et al., *Comparison on the total phenol contents and the color of fresh and infrared dried olive leaves.* Industrial Crops and Products, 2009. **29**(2-3): p. 412-419.
58. Gimeno, E., et al., *The effects of harvest and extraction methods on the antioxidant content (phenolics, a-tocopherol, and b-carotene) in virgin olive oil.* Food Chemistry, 2002. **78**: p. 207-211.
59. El, S.N. and S. Karakaya, *Olive tree (Olea europaea) leaves: potential beneficial effects on human health.* Nutrition Reviews, 2009. **67**(11): p. 632-638.
60. Arslan, D., *Physico-chemical characteristics of olive fruits of Turkish varieties from the province of Hatay.* Grasas y Aceites, 2012. **63**(2): p. 158-166.
61. Juan, M.E., et al., *Olive Fruit Extracts Inhibit Proliferation and Induce Apoptosis in HT-29 Human Colon Cancer Cells.* The Journal of Nutrition, 2006. **136**(10): p. 2553-2557.
62. Rodríguez, G., et al., *Olive stone an attractive source of bioactive and valuable compounds.* Bioresource Technology, 2008. **99**(13): p. 5261-5269.
63. Fabiani, R., et al., *Cancer chemoprevention by hydroxytyrosol isolated from virgin olive oil through G1 cell cycle arrest and apoptosis.* European Journal of Cancer Prevention, 2002. **11**(4): p. 351-358.
64. Hamdi, H.K. and R. Castellon, *Oleuropein, a non-toxic olive iridoid, is an anti-tumor agent and cytoskeleton disruptor.* Biochemical and Biophysical Research Communications, 2005. **334**(3): p. 769-778.
65. Bulotta, S., et al., *Biological Activity of Oleuropein and its Derivatives*, in *Natural Products*, K.G. Ramawat and J.-M. Mérillon, Editors. 2013, Springer Berlin Heidelberg. p. 3605-3638.
66. Gao, K., et al., *Comparative Study of Activities between Verbascoside and Rutin by Docking Method.* QSAR & Combinatorial Science, 2003. **22**(1): p. 18-28.
67. Li, J., et al., *Differentiation of human gastric adenocarcinoma cell line MGc80-3 induced by verbascoside.* Planta Med, 1997. **63**(6): p. 499-502.
68. Patel, D., S. Shukla, and S. Gupta, *Apigenin and cancer chemoprevention: progress, potential and promise (review).* Int J Oncol, 2007. **30**(1): p. 233-45.
69. Horinaka, M., et al., *The dietary flavonoid apigenin sensitizes malignant tumor cells to tumor necrosis factor–related apoptosis-inducing ligand.* Molecular Cancer Therapeutics, 2006. **5**(4): p. 945-951.
70. Manthey, J.A. and G. Najla, *Antiproliferative Activities of Citrus Flavonoids against Six Human Cancer Cell Lines.* J. Agric. Food Chem., 2002. **50**: p. 5837-5843.

71. Wu, B., et al., *Anti-proliferative and chemosensitizing effects of luteolin on human gastric cancer AGS cell line.* Molecular and Cellular Biochemistry, 2008. **313**(1-2): p. 125-132.
72. Lin, Y., et al., *Luteolin, a flavonoid with potential for cancer prevention and therapy.* Curr Cancer Drug Targets, 2008. **8**(7): p. 634-46.
73. Morley, K.L., P.J. Ferguson, and J. Koropatnick, *Tangeretin and nobiletin induce G1 cell cycle arrest but not apoptosis in human breast and colon cancer cells.* Cancer Letters, 2007. **251**(1): p. 168-178.
74. YOSHIMIZU, N., et al., *Anti-tumour effects of nobiletin, a citrus flavonoid, on gastric cancer include: antiproliferative effects, induction of apoptosis and cell cycle deregulation.* Aliment Pharmacol Ther, 2004. **20**: p. 95-101.
75. Lin, N., et al., *Novel anti-inflammatory actions of nobiletin, a citrus polymethoxy flavonoid, on human synovial fibroblasts and mouse macrophages.* Biochemical Pharmacology, 2003. **65**(12): p. 2065–2071.
76. Chen, Z.-T., et al., *Protective effects of sweet orange (Citrus sinensis) peel and their bioactive compounds on oxidative stress.* Food Chemistry, 2012. **135**(4): p. 2119-2127.
77. Li, S., et al., *Chemistry and health effects of polymethoxyflavones and hydroxylated polymethoxyflavones.* Journal of Functional Foods, 2009. **1**(1): p. 2-12.
78. Park, H.J., et al., *Apoptotic effect of hesperidin through caspase3 activation in human colon cancer cells, SNU-C4.* Phytomedicine, 2008. **15**(1–2): p. 147-151.
79. Lee, K.-H., et al., *The inhibitory effect of hesperidin on tumor cell invasiveness occurs via suppression of activator protein 1 and nuclear factor-kappaB in human hepatocellular carcinoma cells.* Toxicology Letters, 2010. **194**(1–2): p. 42-49.
80. Zarebczan, B., et al., *Hesperetin, a potential therapy for carcinoid cancer.* The American Journal of Surgery, 2011. **201**(3): p. 329-333.
81. Choi, E.J., *Hesperetin induced G1-phase cell cycle arrest in human breast cancer MCF-7 cells: involvement of CDK4 and p21.* Nutr Cancer, 2007. **59**(1): p. 115-9.
82. Lentini, A., et al., *Enhancement of transglutaminase activity and polyamine depletion in B16-F10 melanoma cells by flavonoids naringenin and hesperitin correlate to reduction of the in vivo metastatic potential.* Amino Acids, 2007. **32**(1): p. 95-100.
83. Dong, Y., et al., *[Effects of sinensetin on proliferation and apoptosis of human gastric cancer AGS cells].* Zhongguo Zhong Yao Za Zhi, 2011. **36**(6): p. 790-4.
84. Lam, I.K., et al., *In vitro and in vivo structure and activity relationship analysis of polymethoxylated flavonoids: identifying sinensetin as a novel antiangiogenesis agent.* Mol Nutr Food Res, 2012. **56**(6): p. 945-56.
85. Totta, P., et al., *Mechanisms of Naringenin-induced Apoptotic Cascade in Cancer Cells: Involvement of Estrogen Receptor α and ß Signalling.* IUBMB Life, 2004. **56**(8): p. 491-499.
86. Tomás-Barberán, F.A., et al., *HPLC-DAD-ESIMS Analysis of Phenolic Compounds in Nectarines, Peaches, and Plums.* J. Agric. Food Chem., 2001. **49**: p. 4748-4760.
87. Usenik, V., J. Fabčič, and F. Štampar, *Sugars, organic acids, phenolic composition and antioxidant activity of sweet cherry (Prunus avium L.).* Food Chemistry, 2008. **107**(1): p. 185-192.
88. Murillo, E., A.J. Meléndez-Martínez, and F. Portugal, *Screening of vegetables and fruits from Panama for rich sources of lutein and zeaxanthin.* Food Chemistry, 2010. **122**(1): p. 167-172.
89. Kim, Y.-N., D.W. Giraud, and J.A. Driskell, *Tocopherol and carotenoid contents of selected Korean fruits and vegetables.* Journal of Food Composition and Analysis, 2007. **20**(6): p. 458-465.
90. Serra, A.T., et al., *Processing cherries (Prunus avium) using supercritical fluid technology. Part 2. Evaluation of SCF extracts as promising natural chemotherapeutical agents.* The Journal of Supercritical Fluids, 2011. **55**(3): p. 1007-1013.

91. Khoo, G.M., et al., *Bioactivity and total phenolic content of 34 sour cherry cultivars.* Journal of Food Composition and Analysis, 2011. **24**(6): p. 772-776.
92. Gao, L. and G. Mazza, *Characterization, quantitation, and distribution of anthocyanins and colorless phenolics in sweet cherries.* Journal of Agricultural and Food Chemistry, 1995. **42**: p. 343-346.
93. YAO, L.H., et al., *Flavonoids in Food and Their Health Benefits.* Plant Foods for Human Nutrition, 2004. **59**: p. 113–122.
94. CHAOVANALIKIT, A. and R.E. WROLSTAD, *Total Anthocyanins and Total Phenolics of Fresh and Processed Cherries and Their Antioxidant Properties.* Food Chemistry and Toxicology, 2003.
95. Zhang, Y., S.K. Vareed, and M.G. Nair, *Human tumor cell growth inhibition by nontoxic anthocyanidins, the pigments in fruits and vegetables.* Life Sciences, 2005. **76**(13): p. 1465–1472.
96. Kang, S.-Y., et al., *Tart cherry anthocyanins inhibit tumor development in ApcMin mice and reduce proliferation of human colon cancer cells.* Cancer Letters, 2003. **194**(1): p. 13-19.
97. Blando, F., C. Gerardi, and I. Nicoletti, *Sour Cherry (Prunus cerasus L) Anthocyanins as Ingredients for Functional Foods.* Journal of Biomedicine and Biotechnology, 2004. **5**: p. 253-258.
98. Bardon, S., et al., *Monoterpenes inhibit proliferation of human colon cancer cells by modulating cell cycle-related protein expression.* Cancer Letters, 2002. **181**: p. 187-194.
99. Loutrari, H., *Perillyl Alcohol Is an Angiogenesis Inhibitor.* Journal of Pharmacology and Experimental Therapeutics, 2004. **311**(2): p. 568-575.
100. Wagner, J.E., et al., *Perillyl Alcohol Inhibits Breast Cell Migration without Affecting Cell Adhesion.* Journal of Biomedicine and Biotechnology, 2002. **2**: p. 136–140.
101. Tanaka, T., T. Tanaka, and M. Tanaka, *Potential Cancer Chemopreventive Activity of Protocatechuic Acid.* Journal of Experimental & Clinical Medicine, 2011. **3**(1): p. 27-33.
102. Shin-ichi, K., et al., *Antioxidant Activity of Prune (Prunus domestica L.) Constituents and a New Synergist.* Journal of Agricultural and Food Chemistry, 2002. **50**.
103. Oliveira, A., M. Pintado, and D.P.F. Almeida, *Phytochemical composition and antioxidant activity of peach as affected by pasteurization and storage duration.* LWT - Food Science and Technology, 2012. **49**(2): p. 202-207.
104. Usenik, V., F. Stampar, and D. Kastelec, *Phytochemicals in fruits of two Prunus domestica L. plum cultivars during ripening.* Journal of the Science of Food and Agriculture, 2013. **93**(3): p. 681-692.
105. Huang, H.-P., et al., *Anthocyanin-rich Mulberry extract inhibit the gastric cancer cell growth in vitro and xenograft mice by inducing signals of p38/p53 and c-jun.* Food Chemistry, 2011. **129**(4): p. 1703-1709.
106. Ribaya-Mercado, J.D. and J.B. Blumberg, *Lutein and zeaxanthin and their potential roles in disease prevention.* J Am Coll Nutr, 2004. **23**(6 Suppl): p. 567S-587S.
107. Yuri, T., et al., *Perillyl alcohol inhibits human breast cancer cell growth in vitro and in vivo.* Breast Cancer Res Treat, 2004. **84**(3): p. 251-60.
108. Lambert, J.D. and C.S. Yang, *Mechanisms of cancer prevention by tea constituents.* J Nutr, 2003. **133**(10): p. 3262S-3267S.
109. Zaveri, N.T., *Green tea and its polyphenolic catechins: medicinal uses in cancer and noncancer applications.* Life Sci, 2006. **78**(18): p. 2073-80.
110. Alonso-Castro, A.J., F. Domínguez, and A. García-Carrancá, *Rutin Exerts Antitumor Effects on Nude Mice Bearing SW480 Tumor.* Archives of Medical Research, (0).
111. Webster, R.P., M.D. Gawde, and R.K. Bhattacharya, *Protective effect of rutin, a flavonol glycoside, on the carcinogen-induced DNA damage and repair enzymes in rats.* Cancer Letters, 1996. **109**(1–2): p. 185-191.

112. Jin, U.H., et al., *A phenolic compound, 5-caffeoylquinic acid (chlorogenic acid), is a new type and strong matrix metalloproteinase-9 inhibitor: isolation and identification from methanol extract of Euonymus alatus.* Life Sci, 2005. **77**(22): p. 2760-9.
113. Noratto, G., et al., *Identifying Peach and Plum Polyphenols with Chemopreventive Potential against Estrogen-Independent Breast Cancer Cells.* Journal of Agricultural and Food Chemistry, 2009. **57**(12): p. 5219-5226.
114. Lin, H.-H., et al., *Protocatechuic acid inhibits cancer cell metastasis involving the down-regulation of Ras/Akt/NF-κB pathway and MMP-2 production by targeting RhoB activation.* British Journal of Pharmacology, 2011. **162**(1): p. 237-254.
115. Tseng, T.-H., et al., *Induction of apoptosis by Hibiscus protocatechuic acid in human leukemia cells via reduction of retinoblastoma (RB) phosphorylation and Bcl-2 expression.* Biochemical Pharmacology, 2000. **60**(3): p. 307-315.
116. Wang, L.-S., et al., *Anthocyanins and Cancer Prevention*, in *Nutraceuticals and Cancer*, F.H. Sarkar, Editor. 2012, Springer Netherlands. p. 201-229.
117. Wang, L.-S. and G.D. Stoner, *Anthocyanins and their role in cancer prevention.* Cancer Letters, 2008. **269**(2): p. 281-290.
118. Steinmetz, K.L. and E.G. Spack, *The basics of preclinical drug development for neurodegenerative disease indications.* BMC Neurology, 2009. **9**(Suppl 1): p. S2.
119. Prasad, S., et al., *Regulation of signaling pathways involved in lupeol induced inhibition of proliferation and induction of apoptosis in human prostate cancer cells.* Molecular Carcinogenesis, 2008. **47**(12): p. 916-924.
120. Gayet, J., et al., *Extensive characterization of genetic alterations in a series of human colorectal cancer cell lines.* Oncogene, 2001. **20**: p. 5025-5032.
121. Kim, J.B., R. Stein, and M.J. O'Hare, *Three-dimensional in vitro tissue culture models of breast cancer – a review.* Breast Cancer Research and Treatment, 2004(85): p. 281-291.
122. Barrila, J., et al., *Organotypic 3D cell culture models: using the rotating wall vessel to study host–pathogen interactions.* Nature Reviews Microbiology, 2010. **8**(11): p. 791-801.
123. Jayme L. Horning, S.K.S., Sivakumar Vijayaraghavalu, Sanja Dimitrijevic, Jaspreet K. Vasir, Tapan K. Jain, Amulya K. Panda, and Vinod Labhasetwar, *3-D Tumor Model for In Vitro Evaluation of Anticancer Drugs.* Molecular Pharmaceutics, 2008. **5**(5): p. 849-862.
124. Ivascu, A. and M. Kubbies, *Rapid Generation of Single-Tumor Spheroids for High-Throughput Cell Function and Toxicity Analysis.* Journal of Biomolecular Screening, 2006. **11**(8): p. 922-932.
125. Mueller-Klieser, W., *Multicellular spheroids: a review on cellular aggregates in cancer research.* J Cancer Res Clin Oncol, 1987. **113**: p. 101-122.
126. Schmeichel, K. and M. Bissell, *Modeling tissue-specific signaling and organ function in three dimensions.* Journal of cell science, 2003. **116**(Pt 12): p. 2377-2388.
127. Mazzoleni, G., D. Di Lorenzo, and N. Steimberg, *Modelling tissues in 3D: the next future of pharmaco-toxicology and food research?* Genes & Nutrition, 2009. **4**(1): p. 13-22.
128. Lin, R.-Z. and H.-Y. Chang, *Recent advances in three-dimensional multicellular spheroid culture for biomedical research.* Biotechnology Journal, 2008. **3**(9-10): p. 1172-1184.
129. Rose G. Harrison, M.J.G., Franklin P. Mall, C. M. Jackson, *Observations of the living developing nerve fiber.* The Anatomical Record, 1907. **1**(5): p. 116–128.
130. Wainer Zoli , L.R., Anna Tesei , Fabio Barzanti , Dino Amadori, *In vitro preclinical models for a rational design of chemotherapy combinations in human tumors.* Critical Reviews in Oncology:Hematology, 2001(37): p. 69-82.
131. Charles H. Streuli, N.B., and Mina J. Bissell, *Control of Mammary Epithelial Differentiation : Basement Membrane Induces Tissue-specific Gene Expression in the Absence of Cell-Cell Interaction and Morphological Polarity.* The Journal of Cell Biology, 1991. **115**.

132. Mueller-Klieser, W., *Tumor biology and experimental therapeutics.* Critical Reviews in Oncology/Hematology, 2000. **36**: p. 123-139.
133. McMahon, K.M., et al., *Characterization of Changes in the Proteome in Different Regions of 3D Multicell Tumor Spheroids.* Journal of Proteome Research, 2012. **11**(5): p. 2863-2875.
134. KLUNDER, I. and D.F. HULSER, *B-Galactosidase Activity in Transfected Ltk- Cells is Differentially Regulated in Monolayer and in Spheroid Cultures.* Experimental Cell Research, 1993. **207**: p. 155-162.
135. Alvarez-Pérez, J., P. Ballesteros, and S. Cerdán, *Microscopic images of intraspheroidal pH by 1H magnetic resonance chemical shift imaging of pH sensitive indicators.* Magnetic Resonance Materials in Physics, Biology and Medicine, 2005. **18**(6): p. 293-301.
136. http://ip3d.itav-recherche.fr/IP3D/Spheroids_imaging.html, accessed on 10/08/2013.
137. Kim, J.B., *Three-dimensional tissue culture models in cancer biology.* Seminars in Cancer Biology, 2005. **15**(5): p. 365-377.
138. Alford, D. and J. Taylor-Papadimitriou, *Cell adhesion molecules in the normal and cancerous mammary gland.* Journal of mammary gland biology and neoplasia, 1996. **1**(2): p. 207-218.
139. Sutherland, R.M., et al., *Oxygenation and Differentiation in Multicellular Spheroids of Human Colon Carcinoma.* CANCER RESEARCH 1986(46): p. 5320-5329.
140. Karlsson, H., et al., *Loss of cancer drug activity in colon cancer HCT-116 cells during spheroid formation in a new 3-D spheroid cell culture system.* Experimental Cell Research, 2012. **318**(13): p. 1577-1585.
141. Lobjois, V., et al., *Cell cycle and apoptotic effects of SAHA are regulated by the cellular microenvironment in HCT116 multicellular tumour spheroids.* European Journal of Cancer, 2009. **45**(13): p. 2402-2411.
142. Vermeulen, L., et al., *Wnt activity defines colon cancer stem cells and is regulated by the microenvironment.* Nat Cell Biol, 2010. **12**(5): p. 468-76.
143. Dolznig, H., et al., *Modeling colon adenocarcinomas in vitro a 3D co-culture system induces cancer-relevant pathways upon tumor cell and stromal fibroblast interaction.* Am J Pathol, 2011. **179**(1): p. 487-501.
144. SUTHERLAND, R.M., *Cell and Environment Interactions in Tumor Microregions: The Multicell Spheroid Model.* Science, 1988. **240**: p. 177-184.
145. Kim, J., R. Stein, and M. O'Hare, *Three-dimensional in vitro tissue culture models of breast cancer-- a review.* Breast cancer research and treatment, 2004. **85**(3): p. 281-291.
146. Ingram, M., et al., *Three-dimensional growth patterns of various human tumor cell lines in simulated microgravity of a NASA bioreactor.* In vitro cellular & developmental biology. Animal, 1997. **33**(6): p. 459-466.
147. Hammond, T. and J. Hammond, *Optimized suspension culture: the rotating-wall vessel.* American journal of physiology. Renal physiology, 2001. **281**(1): p. 25.
148. Breslin, S. and L. O'Driscoll, *Three-dimensional cell culture: the missing link in drug discovery.* Drug Discovery Today, 2013. **18**(5-6): p. 240-249.
149. Ong, S.-M., et al., *A gel-free 3D microfluidic cell culture system.* Biomaterials, 2008. **29**(22): p. 3237-3244.
150. Hutmacher, D.W. and H. Singh, *Computational fluid dynamics for improved bioreactor design and 3D culture.* Trends in Biotechnology, 2008. **26**(4): p. 166-172.
151. Zuo, Z. and R. Johns, *Halothane, enflurane, and isoflurane do not affect the basal or agonist-stimulated activity of partially isolated soluble and particulate guanylyl cyclases of rat brain.* Anesthesiology, 1995. **83**(2): p. 395-404.
152. Tan, W., R. Krishnaraj, and T. Desai, *Evaluation of nanostructured composite collagen--chitosan matrices for tissue engineering.* Tissue engineering, 2001. **7**(2): p. 203-210.

153. Nelson, C. and M. Bissell, *Modeling dynamic reciprocity: engineering three-dimensional culture models of breast architecture, function, and neoplastic transformation.* Seminars in Cancer Biology, 2005. **15**(5): p. 342-352.
154. Skardal, A., et al., *The generation of 3-D tissue models based on hyaluronan hydrogel-coated microcarriers within a rotating wall vessel bioreactor.* Biomaterials, 2010. **31**(32): p. 8426-8435.
155. Diogo, J.S.G., *Valorization of wild olives (Olea europaea var. sylvestris) as potential source of functional ingredients.* 2013, Universidade de Lisboa: Lisboa.
156. Toledo-Guillén, A.R., et al., *Extraction of Bioactive Flavonoid Compounds from Orange (Citrus sinensis) Peel Using Supercritical CO2.* Special Abstracts / Journal of Biotechnology, 2010. **150S**: p. S1-S576.
157. Bravo, M.N., et al., *Analysis of phenolic compounds in Muscatel wines produced in Portugal.* Analytica Chimica Acta, 2006. **563**(1–2): p. 84-92.
158. Sambuy, Y., et al., *The Caco-2 cell line as a model of the intestinal barrier: influence of cell and culture-related factors on Caco-2 cell functional characteristics.* Cell Biology and Toxicology 2005. **21**(1): p. 21-26.
159. Frydoonfar, H.R., D.R. McGrath, and A.D. Spigelman, *The variable effect on proliferation of a colon cancer cell line by the citrus fruit flavonoid Naringenin.* Colorectal Disease, 2003. **5**(2): p. 149-152.
160. Ho, K., et al., *Apoptosis and cell cycle arrest of human colorectal cancer cell line HT-29 induced by vanillin.* Cancer Epidemiology, 2009. **33**(2): p. 155-160.
161. Kelm, J.M., et al., *Method for generation of homogeneous multicellular tumor spheroids applicable to a wide variety of cell types.* Biotechnology and Bioengineering, 2003. **83**(2): p. 173-180.
162. Wan Yong Ho, S.K.Y., Chai Ling Ho, Raha Abdul Rahim, Noorjahan Banu Alitheen, *Culture from Breast Cancer Cell and a High Throughput Screening Method Using the MTT Assay.* PLOS ONE, 2012. **7**(9): p. 1-6.
163. Fan, X., et al., *Isolation and characterization of spheroid cells from the HT29 colon cancer cell line.* International Journal of Colorectal Disease, 2011. **26**(10): p. 1279-1285.
164. Serra, M., et al., *Process engineering of human pluripotent stem cells for clinical application.* Trends in Biotechnology, 2012. **30**(6): p. 350-359.
165. Wong, K., U. Rubenthiran, and S. Jothy, *Motility of colon cancer cells: modulation by CD44 isoform expression.* Experimental and Molecular Pathology, 2003. **75**(2): p. 124-130.
166. Dalerba, P., et al., *Phenotypic characterization of human colorectal cancer stem cells.* Proceedings of the National Academy of Sciences, 2007. **104**(24): p. 10158-10163.
167. Mittal, S., R. Mifflin, and D.W. Powell, *Cancer stem cells: the other face of Janus.* Am J Med Sci, 2009. **338**(2): p. 107-12.
168. Chen, K.-l., et al., *Highly enriched CD133+CD44+ stem-like cells with CD133+CD44high metastatic subset in HCT116 colon cancer cells.* Clinical & Experimental Metastasis, 2011. **28**(8): p. 751-763.
169. White, S.R., et al., *Initiation of apoptosis by actin cytoskeletal derangement in human airway epithelial cells.* Am J Respir Cell Mol Biol, 2001. **24**(3): p. 282-94.
170. Rufino-Palomares, E.E., et al., *Maslinic acid, a triterpenic anti-tumoural agent, interferes with cytoskeleton protein expression in HT29 human colon-cancer cells.* Journal of Proteomics, 2013. **83**: p. 15-25.
171. Zhu, Q.S., et al., *Vimentin is a novel AKT1 target mediating motility and invasion.* Oncogene, 2010. **30**(4): p. 457-470.
172. Brabletz, T., et al., *Variable -catenin expression in colorectal cancers indicates tumor progression driven by the tumor environment.* Proceedings of the National Academy of Sciences, 2001. **98**(18): p. 10356-10361.

173. Conacci-Sorrell, M., *Autoregulation of E-cadherin expression by cadherin-cadherin interactions: the roles of -catenin signaling, Slug, and MAPK.* The Journal of Cell Biology, 2003. **163**(4): p. 847-857.
174. Owaribe, K., R. Kodama, and G. Eguchi, *Demonstration of contractility of circumferential actin bundles and its morphogenetic significance in pigmented epithelium in vitro and in vivo.* The Journal of Cell Biology, 1981. **90**(2): p. 507-514.
175. Feigin, M.E. and S.K. Muthuswamy, *Polarity proteins regulate mammalian cell–cell junctions and cancer pathogenesis.* Current Opinion in Cell Biology, 2009. **21**(5): p. 694-700.
176. Huber, F., et al., *Emergent complexity of the cytoskeleton: from single filaments to tissue.* Advances in Physics, 2013. **62**(1): p. 1-112.
177. McInroy, L. and A. Määttä, *Down-regulation of vimentin expression inhibits carcinoma cell migration and adhesion.* Biochemical and Biophysical Research Communications, 2007. **360**(1): p. 109-114.
178. Higgins, D.F., et al., *Hypoxia promotes fibrogenesis in vivo via HIF-1 stimulation of epithelial-to-mesenchymal transition.* J Clin Invest, 2007. **117**(12): p. 3810-20.
179. Sundin, T., et al., *The isoprenoid perillyl alcohol inhibits telomerase activity in prostate cancer cells.* Biochimie, 2012. **94**(12): p. 2639-2648.
180. Kaufmann, S., *Induction of Apoptosis by Cancer Chemotherapy.* Experimental Cell Research, 2000. **256**(1): p. 42-49.
181. Yeruva, L., et al., *Perillyl alcohol and perillic acid induced cell cycle arrest and apoptosis in non small cell lung cancer cells.* Cancer Letters, 2007. **257**(2): p. 216-226.
182. Promega Corporation. Celltiter 96® Aqueous One Solution Cell Proliferation Assay. In Promega Corporation, 2012.
183. Life technologies. PrestoBlue® Cell Viability Reagent. In Life technologies, 2012.

6 Appendix

Appendix A – Cellular viability assays

- CellTiter 96® Aqueous One Cell Proliferation Assay

The CellTiter 96® Aqueous One Cell Proliferation Assay is a colorimetric method used in proliferation or cytotoxicity assays for determining the number of viable cells. This assay contains MTS tetrazolium compound (3-(4,5-dimethylthiazol-2-yl)-5-(3-carboxymethoxyphenyl)-2-(4-sulfophenyl)-2H-tetrazolium, inner salt), which is bioreduced by cells into a colored formazan product soluble in culture medium [182].

Methodology:
It was added 100 µl of MTS solution (16.6% MTS in RPMI culture medium with 0.5% of FBS) was added to each well, after medium removal. Cells were incubated with MTS solution for 4 hours at 37 ^{0}C in a humidified, 5% CO_2 atmosphere and the absorbance was read in a 96-well plate reader at 490 nm.

- PrestoBlue® Cell Viability Reagent

PrestoBlue® Cell Viability Reagent is a reagent for rapidly evaluating the viability and proliferation of a wide range of cell types. This is a nonfluorescent resazurin-based solution which is quickly reduced by metabolic active cells giving a quantitative measure of cell proliferation and viability. When it is reduced by viable cells, the PrestoBlue becomes highly fluorescent. Using this cell viability method, the assayed cells can be recovered for further culturing or use in a subsequent assay [183].

Methodology:
After removed the culture medium, it was added 100 µl of PrestoBlue® solution (10% of PrestoBlue® reagent in RPMI culture medium with 0.5% of FBS) to each well. Cells were incubated at 37 ^{0}C in a humidified, 5% CO_2 atmosphere for 2 hours. Finally, the fluorescence was measured in a 96-well plate reader at 580 nm for excitation and 595 nm for emission detection.
In Figure 6.1 are presented the standard curves of two viability methods tested in HT29 spheroids with different sizes and seeded at different concentrations.

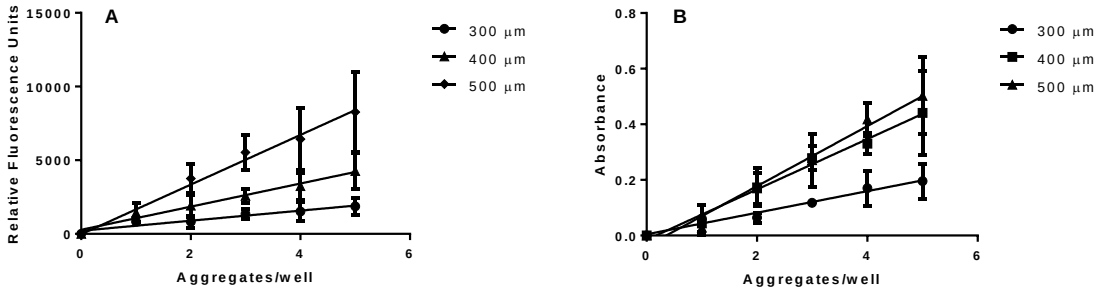

Figure 6.1: (A) Standard curves for PrestoBlue® regent (300 µm – r^2=0.9315; 400 µm – r^2=0.9767; 500 µm – r^2=0.9845) and for (B) CellTiter 96 Aqueous One Cell Proliferation Assay (300 µm – r^2=0.9930; 400 µm – r^2=0.9426; 500 µm – r^2=0.9754) using different HT29 spheroid number per well. Different spheroids sizes were used.

PrestoBlue® was the selected method for the evaluation of cell viability in the 3D model, since the CellTiter 96® method lacks linearity for spheroids of greater diameter. Thus, PrestoBlue appeared to be the most linear method to be used in further assays.

Appendix B – TLC analysis

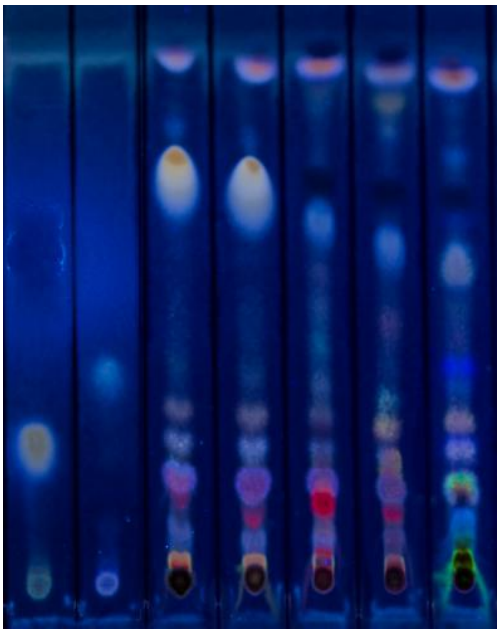

Figure 6.2: TLC analysis of natural extracts obtained by high pressure extraction to reveal terpenes. Legend: 1- perillyl alcohol standard; 2- Linalool standard; 3- Brooks cherry; 4- Sweet Hearth cherry; 5- plum; 6- peach; 7- Orange peel.

Appendix C – Structure of compounds

Table 6.1: Structure of the main compounds present in natural extracts of orange peel and cherry

Sinensetin	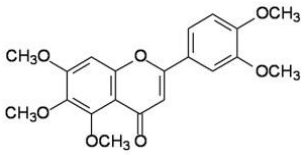
Nobiletin	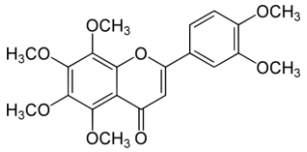
Tangeretin	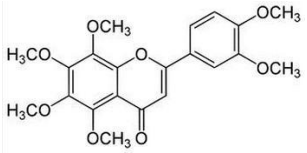
Perillyl alcohol